EXTENDING THE LIFE OF CONCRETE STRUCTURES USING GLYCEROL AS A NANOVISCOSITY MODIFIER: PROTECTION OF REINFORCEMENT STEEL BY REDUCING CHLORIDE TRANSPORT

A Thesis

Presented in Partial Fulfillment of the Requirements for the
Degree of Master of Science
with a
Major in Material Science and Engineering
in the
College of Graduate Studies
University of Idaho
by

Robert D. Blair

Major Professor: Batric Pesic, Ph.D.

Committee Members: Kirshnan Raja, Ph.D.; James Moberly, Ph.D.

Department Administrator: Eric Aston, Ph.D.

May 2017

AUTHORIZATION TO SUBMIT THESIS

This thesis of Robert D. Blair, submitted for the degree of Master of Science with a major in Material Science and Engineering and titled "EXTENDING THE LIFE OF CONCRETE STRUCTURES USING GLYCEROL AS A NANOVISCOSITY MODIFIER: PROTECTION OF REINFORCEMENT STEEL BY REDUCING CHLORIDE TRANSPORT," has been reviewed in final form. Permission, as indicated by the signatures and dates below, is now granted to submit final copies to the College of Graduate Studies for approval.

Major Professor: _____ Date: _____
Batric Pesic, Ph.D.

Committee Members: _____ Date: _____
Krishnan Raja, Ph.D.

_____ Date: _____
James Moberly, Ph.D.

Department
Administrator: _____ Date: _____
Eric Aston, Ph.D.

ABSTRACT

An emerging issue for nuclear energy is correct storage of spent nuclear fuel. Current storage of radioactive waste involves highly durable concrete containment units. The overall strength of concrete and amount of protection it offers its rebar reinforcement is dependent on concrete's microstructure. If moisture easily permeates the microstructure, allowing chloride ion diffusion, the steel rebar is at risk of corrosion. Upon corrosion of the reinforcement steel, a concrete structures service life begins to decline.

Glycerol as a nanoscale viscosity modifier was used to control transport phenomena in the conductive pathways. Increasing moisture viscosity within pore pathways effectively slows diffusion of chloride ions. This study examines admixture effect on moisture transport phenomena (permeability) through concrete conductive pathways (concrete pores). Simultaneously, glycerol admixtures effect on embedded reinforcement steel corrosion was characterized. Permeability was measured using direct measurement techniques while effect of glycerol on rebar corrosion was electrochemically analyzed.

ACKNOWLEDGMENTS

I would first like to thank my major professor Dr. Batric Pesic. The professor's knowledge concerning electrochemistry and its application towards material science is considerable. Dr. Pesic is always able to bring out the best in his students. His motivation inspired me to pursue graduate studies, the experience has truly been rewarding. Without Dr. Pesic's mentorship and guidance this thesis would not have been possible.

Additional recognition must go out to the remaining research team members. I would like to express my appreciation to Dr. Krishnan Raja, whose input and suggestions were always insightful and directed towards the success of the project and students involved. The cooperative support from my fellow graduate researches Jacob Kline and Ian Ehrsam should not be overlooked. Thanks, to Jake and Ian for their encouragement as well as their share in the hard work.

A final, but no less important, acknowledgment goes to the U.S. Department of Energy for funding the research through the Nuclear Energy Universities Programs (NEUP PROGRAM, Contract No. DE-NE0000659-003).

DEDICATION

This work is dedicated in part to both family and friends.

TABLE OF CONTENTS

LIST OF FIGURES

LIST OF TABLES

CHAPTER 1

INTRODCUTION

Cement and concrete are the most common building materials in the world and have been used for thousands of years.[1] The flat grey walls of a building or the smooth pillars of a bridge give an initial impression of simplicity, however the cement and concrete matrix is quite complex.

Concrete is primarily composed of three main constituents, a mortar binding material, sand and/or rock aggregate, and water. Upon mixing of these materials, workable slurry is formed. This concrete slurry can be poured into molds of almost any shape and size where it will harden over time. The resulting structures will be compressively strong, chemically resistant, and effectively insoluble in water. This versatility makes concrete very appealing as a building material.

The mechanical and physical properties of concrete are applied in a variety of constructions including skyscrapers, bridges, side-walks and roads. Concrete has also been used in the design of secondary containment units for nuclear reactors and radioactive waste management. The previously designated long term storage facility inside Yucca Mountain was effectively canceled in 2009. [2] Without a permanent long term storage facility in the United States, nuclear waste must be stored on-site. For on-site storage concrete is used as an encasement material for dry storage casks of spent radioactive fuel. Concrete is very strong but has some fundamental issues. In regards to the environmental degradation which would occur from the failure of a nuclear waste storage cask, these fundamental issues must be addressed. There are two fundamental issues 1) concrete is permeable to moisture and 2) has comparatively low tensile strength.

Concrete is porous which leads to moisture uptake. In colder environments, this is a problem due to freeze thaw cycles. Water seeps into concrete over spring and summer months and then freezes and expands during winter periods. Internal expansion induces tensile strain on the outer surface of the concrete, this leads to strain induced spalling. Furthermore, in colder regions the use of deicing salts which contain chloride ions can cause accelerated corrosion of reinforcement steel, leading to concretes second major problem.

Concrete does not have great tensile strength. Concrete tensile strength (~2-3MPa) is about 10% of its compressive strength (~42MPa). [3] When exposed to tensile strain, concrete is brittle and prone to fracture. The use of reinforcement steel (rebar) in concrete has become common practice. The steel reinforcements are often rod shaped and can be formed into tight grids. These steel grids can be pre-

tensioned prior to concrete casting or post-tensioned once concrete has set. The tensioning of steel induces compressive forces within the concrete negating tensile strain.

Unfortunately, moisture provides a conduit medium for arrival to the rebar surface of deleterious species, such as chloride (Cl^-) and carbonic acid (HCO_3^-). When exposed to chloride the reinforcement steel will undergo a catalytic corrosion of iron. Corrosion reaction products are larger in volume then the original iron atoms. Carbon dioxide initiates pH reduction by carbonation within the concrete pore medium. As pH declines the steel's defense against corrosion weakens. As these reactions progress the internal expansion of corrosion products, much like during the freeze thaw cycle, induce added stress within the concrete leading to spalling and in more dramatic cases mechanical or structural failure. Therefore, it can be said that the overall life time of a concrete structure is based on its resistance to moisture uptake. Reduced moisture uptake will correspond to less moisture ingress and better protection of steel reinforcement.

Conceptually, reduction in moisture permeability will correspond with diminished chloride and carbon dioxide presence. Restrained permeability can be achieved by modifying the size and density of concrete pores. Pozzolanic materials such as fly ash, blast furnace slag or fumed silica are common additives to concrete. These materials are used because they take part in hydration reactions, effectively reducing pore volume and augmenting concrete density.[4][5] Although these admixtures have been proven effective at protecting the reinforcement from chlorides, alternative methods have been suggested and deserve further study.

Bentz et.al proposed that a concrete structure's lifetime could be doubled by increasing moisture viscosity within the porous pathways. [6] [7] This novel approach differs from more standard practices. Application of a viscosity modifier is unique since ionic ingress is reduced without physically changing pore diameter.

Glycerol, a viscous non-toxic sugar tri-alcohol, and its derivatives has been used across a variety of industrial applications. [8] It has been serviced in food products as both a sweetener and emulsifier. Glycerol can also be found in soap and other toiletry items. Recently an increase in its production has occurred as a byproduct of the biodiesel industry. [9] In this respect, admixture application in concrete would be an elegant alternative use for surplus glycerol.

This project focused its main efforts on decreasing the transport within concrete to prolong service life of concrete. Permeability reduction in concrete was the prime objective. Modulation of concretes pore environment was accomplished via additions of glycerol. It is believed glycerol serves

as a viscosity modifier to the concrete pore solution. The increased viscosity should slow moisture ingress and restricts movement of deleterious ions or molecules through the porous pathways.

The other effort centered on improving techniques for measuring transport within concrete. Mass transfer in concrete is a very slow process, and thus difficult to measure. Several new and nondestructive methods utilizing traditional electrochemistry techniques were developed for this purpose.

CHAPTER 2

C-S-H CHEMISTRY, CONCRETE POROSITY, CAPILARRY TRANSPORT AND DIFFUSION

2.1 C-S-H Chemistry

Of the three main components of concrete, the powdered cement serves as the binding material. Cement is characterized by its mineral content; thus a variety of different cements exist. Depending on which minerals are present and in what quantity, the resulting mechanical properties will be different. The most common cement is Portland cement, sense Portland cement was used during the research it will be the focus of the discussion.

The main component in Portland cement is calcium oxide, followed by silica. Aluminum oxides and iron oxides are also present but in smaller amounts. There are also trace amounts of magnesium oxide, potassium oxide, sodium oxide, and sulfur trioxide.

Table 2.1 Chemical composition of Portland cement. [10]

Constituent	Content [%]
CaO	60-66
SiO_2	20-24
Al_2O_3	4-8
Fe_2O_3	1.5-4
MgO	0.5-2
$Na_2O + K_2O$	0.8-1.5
SO_3	1-3.5

The individual oxides within the powdered cement phase rarely exist singularly, instead forming mineral combinations with each other. Cement is manufactured via calcination of limestone ($CaCO_3$) to produce slack lime (CaO). By combining slack lime with silica, the key minerals alite ($3CaO{\cdot}SiO_2$) and belite ($2CaO{\cdot}SiO_2$) are formed, Table 2.2. This process is referred to as clinkering which uses a large rotary kiln to process and mix components.

Table 2.2 Mineral content of cement. [8]

Constituent	Content [%]
Tricalcium silicate (alite)	63
Dicalcium silicate (belite)	20
Tricalcium aluminate	8
Calcium aluminate ferrite	7
Free CaO	< 1

When cement powder and water are mixed a series of hydration reactions take place in which the mineral components consume the water forming what is referred to as C-S-H gel. The C-S-H gel will initially form around the alite grains of the cement.

$$2(3CaO{\cdot}SiO_2) + 6H_2O = 3CaO{\cdot}2SiO_2{\cdot}3H_2O + 3Ca(OH)_2 \qquad (2.1)$$

Water reaction with belite mineral forms the same C-S-H complex.

$$2(2CaO{\cdot}SiO_2) + 4H_2O = 3CaO{\cdot}2SiO_2{\cdot}3H_2O + Ca(OH)_2 \qquad (2.2)$$

By convention C-S-H terminology, uses C = CaO, Si = SiO_2, A = Al_2O_3, F = Fe_2O_3 and H = H_2O.Thus, the reaction product $3CaO{\cdot}2SiO_2{\cdot}3H_2O$could be written as $C_3S_2H_3$ or just simply C-S-H. Aluminate phase will also undergo reactions with water and gypsum ($CaSO_4{\cdot}2H_2O$) to form ettringite $3CaO{\cdot}Al_2O_3 3CaSO_4{\cdot}32H_2O$, however in regards to the bulk of the system the extent of this reaction is limited, so CaO based minerals will be the main focus.

As hydration continues, cement powder will steadily be consumed by the reactions described above. As cement particles are consumed in production of solid products there is a net decrease in volume. This chemical shrinkage occurs because the volume of solid products is less than initial cement powder and water, but the solid products are larger than the initial C_3S and C_2S. [11]These reactions take place in stages; there is an initial period of high reaction rate over the first few hours after mixing, followed by a period of slow reaction rate during which the cement fully hardens. The second period can be referred to as curing time; the curing time is usually very long (at least one month). As reactions come to completion the water filled space between the mineral particles is slowly filled in by solid C-S-H product.

The space which is not fully filled in by C-S-H product is referred to as capillary pore space. The solution present in this space is simply referred to as pore solution. Note pore solution contains

portions of ions from the minerals present in the cement powder. The pore solution also contains Portlandite ($Ca(OH)_2$).

2.2 Concrete Porosity

The previous section outlined the basic process through which cement forms capillary pores. In addition to these capillary pores, the C-S-H phase itself is porous and contains very small holes (nanometers in size). Furthermore, aggregates of various sizes can be added to cement increasing strength and saving cost. With the addition of sand and/or gravel aggregate, the overall porosity of the concrete is no longer restricted to just the cement medium. The aggregates themselves can be porous in nature and a small boundary exists between the aggregate grain and the cement phase. This boundary is called the interfacial transition zone (ITZ). [12] It's simplest to view overall porosity of concrete as the sum porosity from sand, aggregate, ITZ, capillary pores, and cement pores as outlined in Fig. 2.1.

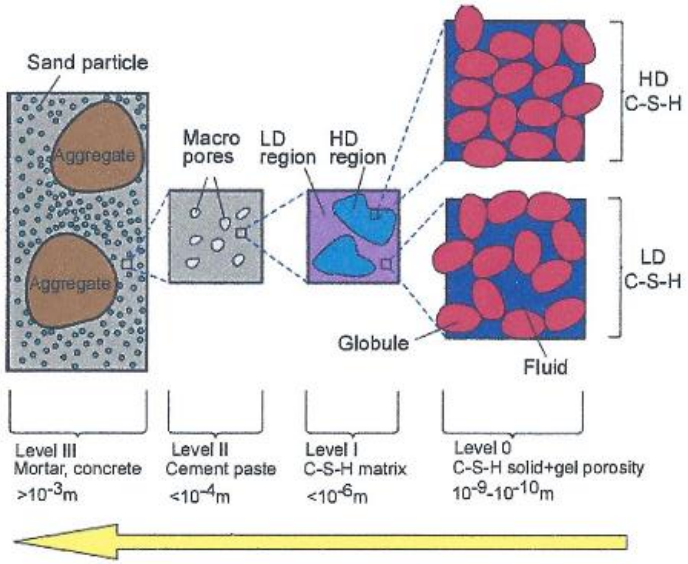

Fig. 2.1 Different components of cement porosity. Scaled images for aggregate, sand and C-S-H phases. High (HD) and low (LD) density porous networks exhibited. [9]

The pores within the C-S-H product are approximately 10^{-9}m. The diameters of capillary pores are micrometers in size ranging from 10^{-6} to 10^{-5}m. The ITZ zones are about 10^{-5} m in width. It should also be mentioned that even larger pores can form because of air entrapment; these can be millimeters in size ranging from 10^{-4} to 10^{-3}m in diameter. [8]

The continuity of porous pathways can be divided into three separate categories as laid out by Song, Fig. 2.2. [13]

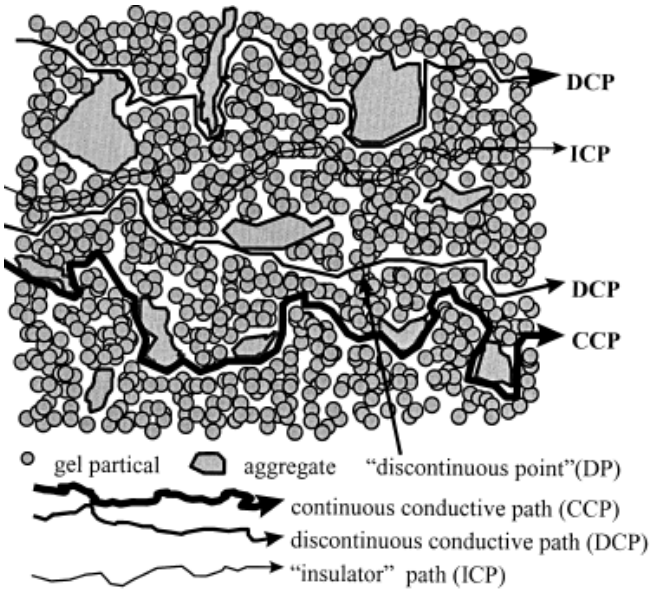

Fig. 2.2 Song's diagram for continuous, discontinuous and insulating porous pathways through concrete.

A porous pathway can be continuous, meaning a series of capillary, ITZ, and air entrapment pores that are interconnected and provide a direct pathway for moisture incursion through the concrete to the rebar. The second possible network is a series of discontinuous pores. An example of this would be two capillary pores separated by C-S-H gel. The small pores within the C-S-H gel still provide means for moisture ingress but in limited amounts. The last possible pathway for moisture incursion, Song refers to as an insulator path. This path would be migration only through the small pores within the C-S-H phase. By far the easiest pathway for moisture and therefore chloride diffusion is through the continuously connected networks.

2.3 Capillary Transport and Diffusion

There are two major mechanisms governing chloride ion navigation through concrete. [8][14] The primary mechanism is by capillary uptake. Chloride can be fully dissolved in water as an ion or not fully dissolved as a crystal salt. As the moisture travels through the cement pores by capillary action, the chloride will be physically towed along by advection.

The second mechanism, diffusion, is for a fully saturated concrete system. This is when both continuous and discontinuous porous channels are full of moisture. In this case, the chloride diffusion

will be driven by chemical potential or the movement from high concentration to lower concentration. Secondary to this is chloride diffusion by charge attraction, movement from negative electric field to positive electric field. The addition of glycerol to the pore solution had an effect on either one or both of the Chloride transport mechanisms, see Experimental Results and Discussion.

CHAPTER 3

CORROSION OF REBAR IN CONCRETE, ELECTROCHEMICAL METHODS FOR STUDYING CORROSION

3.1. Corrosion of Rebar in Concrete

Passivation or passivity is a term describing the relative resistance of metals to oxidation in corrosive environments. Passivation is synonymous with formation of an oxide film on the surface of the metal, oxide films being more tenacious in defense of the metallic surface than insoluble compounds formed by dissolution or precipitation. [15]

Iron is the most extensively used metal for technological applications in human history. Characterization of iron and its alloys, first among them being steel, has been well studied and characterized. Rebar grade steel is low in alloying elements; in particular, it has very little chromium. Chromium, via the formation of Cr_2O_3 layers, is important for increased corrosion resistance in stainless steels. The rebar grade steel used in these studies only contained one alloying element, Manganese, above 1%; the remaining elements were only present in trace amounts. Manganese in small quantities improves high temperature workability of steels. Without the added chromium, the rebar surface's corrosion defense is contingent on the formation of iron oxides.

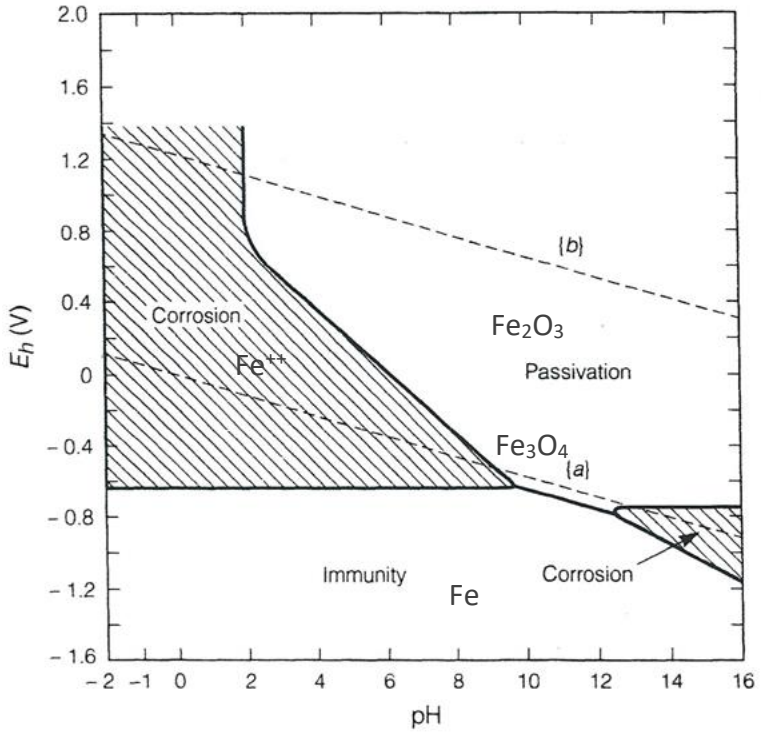

Fig. 3.1 Pourbaix diagrams of iron-water system showing regions of passivation, corrosion and immunity. [15]

The Pourbaix diagram of the Fe-H_2O system, Fig. 3.1, shows the fate of iron as a function of pH and potentials. The dashed lines in the figure represent the stability domain of water. The darker boundary lines represent the various species of iron and iron oxide. These lines correspond to values determined by the Nernst equation.

$$E = E^o + \frac{2.3RT}{nF} log \frac{(A)^a (H^+)^m}{(B)^b (H_2O)^d} \quad (1)$$

The Nernst equation is important because it relates electrochemical potential to Gibbs free-energy exchanged during a reaction. *E* is potential, E^o is the standard potential, *n* is the number of electrons exchanged, *F* is Faradays constant, *R* is the gas constant and *T* is temperature. Once the molar concentrations are known for reactants and products (*A* and *B* respectively) at a given pH (log of H^+ activity), a Pourbaix diagram can be produced for a metal electrolyte system. In this case iron in a concrete pore solution.

Because of C-S-H chemistry, the water in the concrete pore solution is highly alkaline. Leaching of $Ca(OH)_2$, during the curing stage, will set the pH of pore solution to between 12.5-13.5. This high alkaline environment will promote passive film formation on the surface of the embedded steel reinforcement. Referring to Fig. 3.1, at high pH a passive film of iron oxides (Fe_2O_3 and/or Fe_3O_4) will form over a wide range of potentials. [16] The molecular structure of the passive film of iron is generally accepted as being a layer of Fe_3O_4 under an outer layer of γ-Fe_2O_3, however the exact structure of the iron's passive film is still unknown.

Concrete would provide indefinite protection to steel if concrete fully excluded air and water. Unfortunately, as previously mentioned, concrete is porous and these pores serve as conduit pathways for moisture. Moisture inclusion provides a means of arrival for corrosion inducing species such as chloride ions and carbon dioxide (Cl^- and CO_2).

The presence of chloride ions will disrupt the oxide film and initiate localized attack on the steel surface. The hydrolysis of ferrous ions in the presence of chloride ions follows the reaction (3.1).

$$Fe^{2+} + 2H_2O + 2Cl^- \rightarrow Fe(OH)_2 + 2HCl \quad (3.1)$$

This reaction is particularly detrimental to the solid iron, the hydrochloric acid production causes a localized reduction in pH. The acid also serves to accelerate the anodic dissolution of iron into solution. The overall result is an autocatalytic corrosion process in which a self-propagating pit forms underneath the passive film of the iron or steel. During this process, the concentration of chloride in the pit itself will continue to increase while a porous cap of insoluble solid corrosion products precipitates.

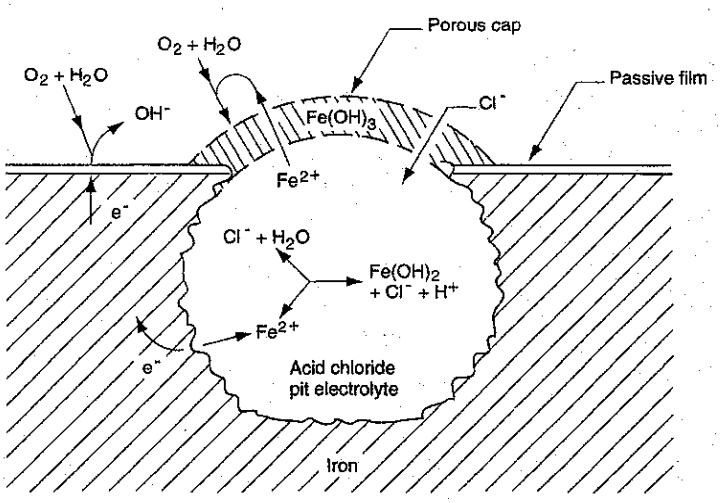

Fig. 3.2 Schematic of processes occurring at an actively growing pit in iron (rebar). [12]

Pitting corrosion is a form of localized corrosion. General corrosion will also be present but influenced more by the amount of CO_2 and dissolved oxygen in the pore solution.

Carbonation reactions threaten passive film stability due to pH reduction.

$$Ca(OH)_2 + CO_2 \rightarrow CaCO_3 + H_2O \quad (3.2)$$

$$H_2O + CO_2 \rightarrow HCO_3^- + H^+ \quad (3.3)$$

The carbonation reactions can lower pore solution pH to as low as pH 9.0, this will greatly weaken mechanisms of passive film formation. As resistance to corrosion declines there will be an increase in corrosion products produced by general corrosion as well as localized corrosion.

Processes of carbonation pH reduction and chloride induced corrosion were replicated experimentally through electrochemical analysis of rebar embedded in concrete. The principle behind this experimental method is that viscosity increase from glycerol admixture will slow the arrival of moisture, chloride and carbon dioxide to the steel surface compared to the non-glycerol control. If this is the case, the initiation of corrosion reactions should occur later and the overall corrosion rates should be slower. The electrochemical techniques applied included open circuit potential (OCP) monitoring, linear polarization (LP), Tafel polarization (Tafel) and cyclic polarization (CP). The principles of these different electrochemical methods are discussed in the following sections.

3.2 Electrochemical Methods for Studying Corrosion

3.2.1 Open Circuit Potential

Open circuit potential also called corrosion potential (E_{corr}), is the equilibrium potential or rest potential for a metal electrolyte system. By far the greatest trait of OCP measurements is simplicity. The corrosion potential measurement is taken without imposed potential and reflects the nature of the electrode (rebar) surface. This potential does not represent a single reaction process but a mixed potential of half-cell reactions from multiple anodic/cathodic cell locations over the entire electrode surface.

When measuring the OCP of reinforcement steel, it is important to emphasize that the OCP value cannot be used to directly interpret a corrosion rate but can be used to detect changes in the condition of the steel being monitored. [17] OCP shifting to anodic potentials then stabilizing is usually indicative of the formation of a passive film while decreasing OCP represents the formation of porous hydroxide layer that merely slows the corrosion process. [18] Sudden cathodic drops in OCP are usually indicative of corrosion activity. In order to measure a current density (corrosion rate) the system must be taken out of equilibrium by an applied potential.

3.2.2 Polarization Methods

Determination of corrosion resistance and corrosion rate requires knowledge of exchange current density. Polarization methods can provide information on corrosion rate, kinetics, and passivation for an electrode in a specific electrolyte at specific times, in this case the degree of current exchange for rebar cylinders in concrete. Fundamentally, the Butler–Volmer relationship can mathematically describe the relationship between current density and applied potential.

$$i = i_{corr}\left\{e^{-\left(\frac{\alpha n F \eta}{RT}\right)} - e^{\left(\frac{(1-\alpha) n F \eta}{RT}\right)}\right\} \qquad (2)$$

Here i is the measured current density resulting from an applied potential, i_{corr} is the corrosion current density of the electrode when it is at OCP, n is the number of electrons exchanged, F is Faradays constant, η is the difference between electrode OCP and applied potential (also called over potential), α is the coefficient (varies between 0 to 1) or fraction of over potential taken for either ionization or discharge in reactions, R is the gas constant and T is temperature. The exponential values exp(-(αnFη/RT) and exp((1-α)nFη/RT) represent cathodic and anodic currents respectively. The main difference between the three main polarization methods of Linear, Tafel, and Cyclic polarization is the degree of applied over potential.

3.2.3 Linear Polarization

Polarization tests use applied voltage as a driving force for reaction and then measure resulting currents. In linear polarization (LP), the current is measured directly against applied potential. The potential is applied in steps, often on the order of mV/s. One advantage to this polarization technique is it can be conducted in a short time frame, commonly less than half an hour, and is non-destructive in nature. Being non-destructive means the tests can be run multiple times on the same electrode without undue influence.

In order not to damage the electrode by causing metal dissolution or buildup of corrosion products, the potential range is kept very small and only varies out from open circuit potential by 25mV in either cathodic or anodic directions. Cathodic direction means more negative potentials than the equilibrium OCP and anodic direction means more positive potentials than the equilibrium OCP. Because the test is run so near the equilibrium state, the currents are often on the order of micro-amps or nano-amps.

An LP graph will display a line with a slope relating change of current vs. potential, Fig. 3.3. This slope is equivalent to polarization resistance R_p.

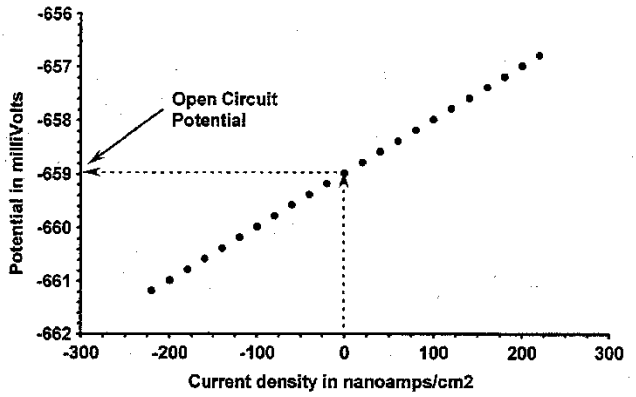

Fig. 3.3 Example linear polarization curve. [15]

The equation for polarization resistance is given, ΔE represents the change in potential and ΔI represents change in current.

$$R_p = \frac{\Delta E}{\Delta I} \qquad (3)$$

Resistance to polarization which has the units of ohms per cm^2 is synonymous with corrosion resistance. The larger the value of R_p measured the greater the resistance to corrosion.

3.2.4 Tafel Polarization

Tafel polarization method functions over a broader potential spectrum then LP and plots current on a log scale. The resulting graph will have two distinct Tafel regions. The two separate branches represent anodic and cathodic half reactions. In a Tafel plot, inflection points from the anodic and cathodic halves specify the values for i_{corr} and E_{corr}, Fig. 3.4a-b.

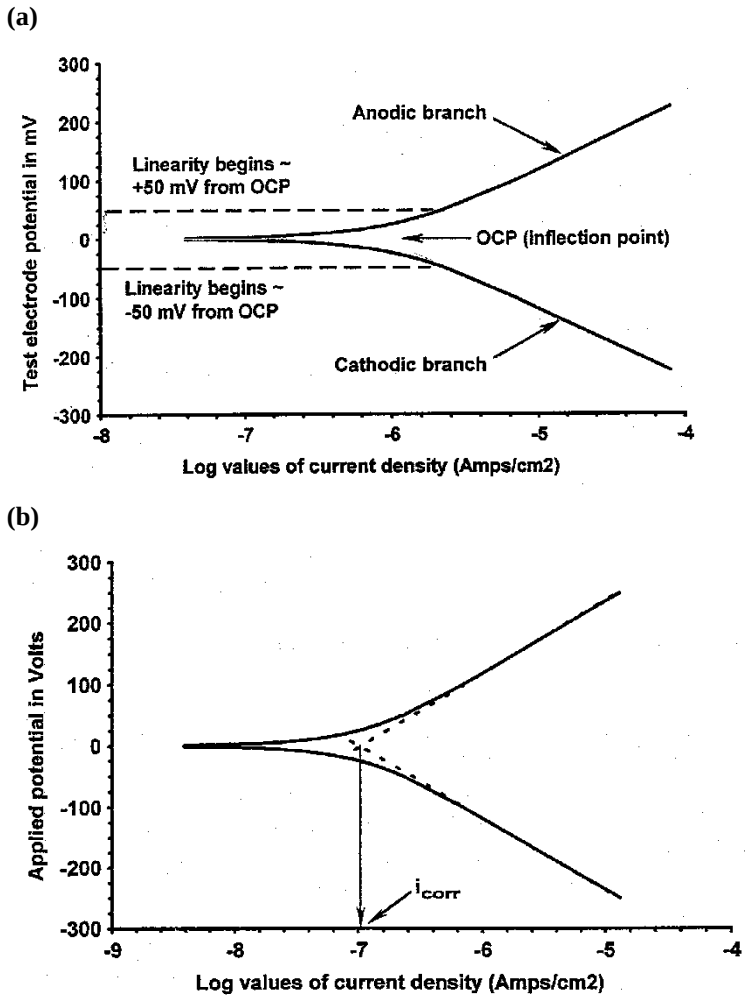

Fig. 3.4 Example interpretations of **(a)** Corrosion potential at the OCP inflection point and **(b)** corrosion current (icorr) from Tafel plots. [15]

For the rebar embedded in concrete, application of the Stern and Geary [19] equation was utilized to solve for polarization resistance R_p, depending on experimentally determined values of i_{corr}, β_a and β_c.

$$i_{corr} = \left(\frac{1}{2.303R_p}\right)\left(\frac{\beta_a\beta_c}{\beta_a+\beta_c}\right) \quad (4)$$

In this equation, the β_a is the slope of the line over one decade of the anodic branch while β_c is the slope of the line over one decade of the cathodic branch. These values, β_a and β_c, are the Tafel constants and equal the over potential expressions given by the Butler-Volmer relationship.

3.2.5 Cyclic Polarization

Potentio-dynamic scans are similar to Linear and Tafel polarizations but apply a much larger range of voltage. Linear polarization scans, as previously mentioned, generally run from -25mV OCP to +25mV OCP and provide basic understanding of the corrosion resistance. Tafel scans run from -250mV OCP to +250mV OCP and provide information on corrosion rate and corrosion potential. The much larger voltage range of a potentio-dynamic scan provides the same information as Tafel but also additional information concerning the protective films. Important information given by potentio-dynamic scanning includes passivation potentials as well as the nature of the corrosion itself be it general or localized. Potentio-dynamic tests can be run in a singular forward scan or can be cyclic with an additional return scan.

In cyclic polarization (CP) the start of the scan mimics Tafel at -250mV vs. OCP. However, after the cathodic branch is complete the potential will extend well past +250mV OCP in the anodic direction, usually on the order of 1 to 2 volts.

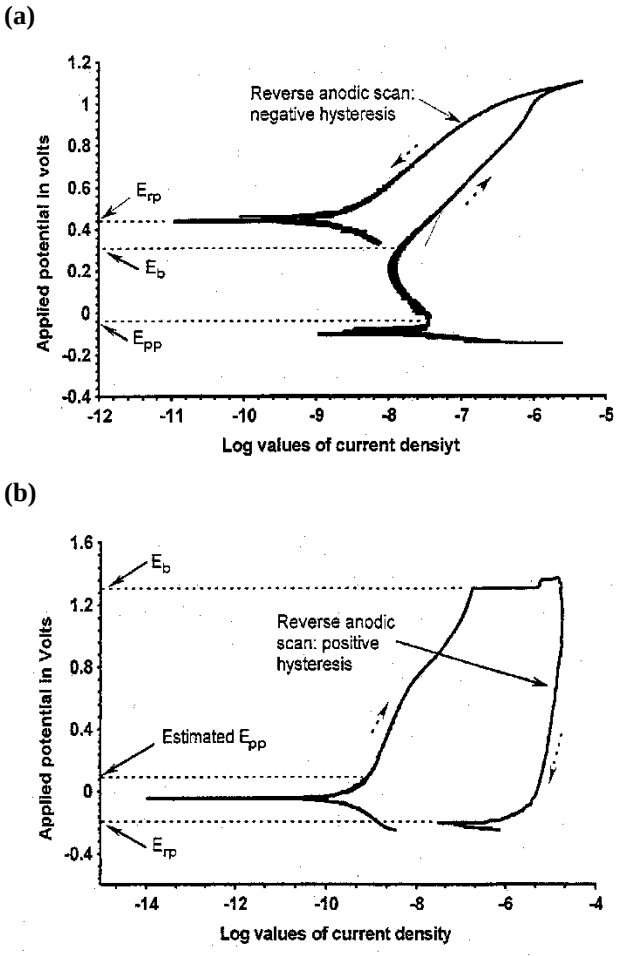

Fig. 3.5 (a) CP curves with negative hysteresis and **(b)** CP curve with positive hysteresis. [15]

There are several important values determined from cyclic polarization plots. One such value is the passive potential range, this is the potential difference between passivation potential E_{pp} to the breakdown potential E_b. The section after the breakdown point is often referred to as the transpassive region. In some cases, as illustrated by Fig 3.5b, passivation potential range can be very small or non-existent. The longer the current remains fixed with increasing potential the greater the passivation potential range and greater the protective film resistance to corrosion. At an experimentally determined point usually one to two decades past the breakdown potential, the scan can be reversed back in the cathodic direction. How the scan returns is very important. If currents decrease with decreasing potential this will result in a negative hysteresis. If currents increase with decreasing potential this will be a positive hysteresis. A negative hysteresis is indicative of no localized corrosion. A positive hysteresis indicates pitting corrosion. In concrete, rebar will undergo localized pitting corrosion when under attack from chloride.

The final important value identified by CP is repair potential. The repair potential shows how readily a protective film reforms after damage. Better performing protective films will repair quickly during a return scan, Fig. 3.5a, while poor protective films will take longer to repair, Fig 3.5b. Note in some cases the return scan with positive hysteresis will cross back through the forward scan. The cross-back point marks the repair potential, see Experimental Results and Discussion.

CHAPTER 4

EXPERIMENTAL TECHNIQUE

4.1 Materials

All concrete and cement castings used a standard Type I/II Portland Cement as binder. The aggregate was 99.4% silica (LM#16 sand) purchased from the Lane Mountain (LnMt) Company of northeastern Washington. Grain size distribution varied from 0.42mm to 1.2mm with the bulk of grains around 0.88mm in size, Table 4.1. The aggregate was treated with a methyl alcohol wash and oven dried to remove possible floating reagents common in sand purification plants.

Table 4.1 Screen analysis of Lane Mt. #16 aggregate

US Screen Size	12	16	20	30	40	pan
Diameter (mm)	---	1.168	0.883	0.589	0.417	---
Grains Retained (%)	0.5	28	60	7.0	2.5	2.5

* Percent retained ±5% per screen

Glycerol ($C_3H_5(OH)_3$) is a hydrophilic sugar alcohol with three functional hydroxyl groups, two primary and one secondary, Fig. 4.1. The anhydrous glycerol was purchased from the J.T. Baker Chemical Company with a formula weight of 92.1 and assay of 100.4.

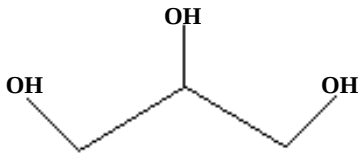

Fig. 4.1 Illustration of glycerol molecular structure.

The reinforcement steel was acquired from Harris Rebar ABCO Meridian Idaho, Nucor Steel in Utah had originally produced the steel. The composition for the steel by element is given in Table 4.2.

Table 4.2 Chemical composition of reinforcement steel.

Element	C	Mn	P	S	Si	Cu	Ni	Cr	Mo	V	Cb	Fe
Wt.%	0.41	1.23	0.017	0.044	0.20	0.25	0.08	0.15	0.019	0.0029	0.001	Balance

4.2 Experimental procedures

4.2.1 Electrochemical cells

The experimental setups for this portion of the project were for corrosion measurements on reinforcement steel (rebar) embedded in concrete cells, Fig. 4.2a-b and Fig. 4.3. The procedure was governed by ASTM C 192/C 192M-06 [20] and involved electrode preparation, solution preparation and corrosion type of measurements in adequately prepared electrochemical cells. For steel embedded in concrete, the procedure involved machining of steel into cylindrical shape, spot welding a lead wire to the cylinder, and protection/insulation of the lead wire and cylinder ends by epoxy and heat shrinkable tubing. At this stage, glass tubes with 2.5mm internal diameter were affixed to the lead wires. The ends of the glass tubes were right in proximity to the edge of the steel cylinders. The prepared electrodes could then be positioned in PVC molds for casting of cement with particular composition.

Table 4.3 Proportions of cement, sand, water and glycerol used in sample preparation.

Admixture (wt.%)	Cement (g)	Sand (g)	Water (ml)	Glycerol (g)	Gly/H_2O (%)
Control Cement Only	100	0	40	0	0
Glycerol 0.5% Cement	100	0	40	0.5	1.25
Glycerol 1.0% Cement	100	0	40	1.0	2.5
Glycerol 2.0% Cement	100	0	40	2.0	5.0
Control + LnMt	50	50	20	0	0
Glycerol 0.5% + LnMt	50	50	20	0.25	1.25
Glycerol 1.0% + LnMt	50	50	20	0.5	2.5
Glycerol 2.0% + LnMt	50	50	20	1.0	5.0

The composition of cement is the key parameter as it reflects the permeability modulation as the function of particular admixture, Table 4.3. Note, the percentage of water to cement binder w/c = 0.4 was kept constant. Each cast was done through incremental layering of concrete. A portion of concrete would be added to the mold and compacted down followed by another portion and subsequent compacting. This progressive compaction method was repeated until the molds were full. The method prevented excessive air entrapment and gradation of sand aggregate or water. Once cast, concrete cells were transferred to curing boxes and allowed to rest for 28 days.

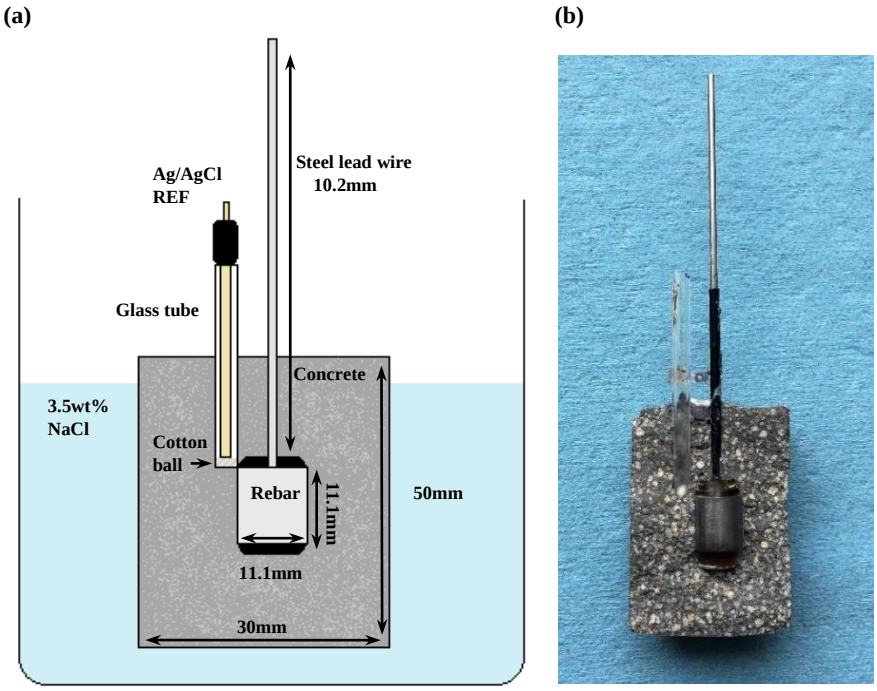

Fig. 4.2 (a) Cross sectional schematic of concrete cell for electrochemical studies. Dimensions of concrete cylinder and rebar electrode labeled. **(b)** Actual cross section of concrete cell with embedded rebar steel for electrochemical studies.

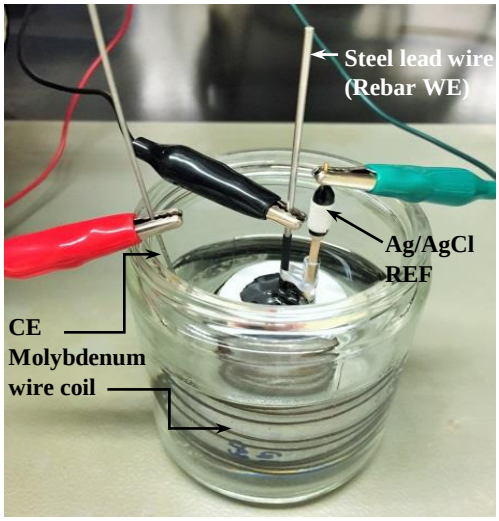

Fig. 4.3 Electrochemical cell during corrosion studies of reinforcement steel (rebar) in concrete. Solution is 3.5 wt.% NaCl. Black AREMCO epoxy covers the top of concrete cylinder.

Some additional things to note, before embedding the electrodes in concrete, the tip of the glass tubing was packed with cotton. The cotton serves a dual purpose, one to prevent cement from filling the end of the tube and second to pull moisture from the concrete matrix and create an ionic bridge between the reference electrode and steel electrode. Furthermore, the tops of the concrete cells were covered with either Marine Weld epoxy or AREMCO epoxy, the epoxy prevented expedient movement of salt solution down the sides of the glass tubing or lead wires.

Moreover, functionality of the Ag/AgCl reference electrodes needed to be verified. It is important to state that the reference electrode (2mm diameter) was of a leak-free type, the important characteristic that ensures the absence of contamination by chloride ions by reference electrode filling solution. However, pH of concrete pore solution can be above pH 13.0 and extremely caustic. There was a possibility that the leak free membrane could be damaged by the high pH. In addition, calcium hydroxides and calcium carbonates within the pore solution could crystallize within the membrane of the electrode. Therefore, a second electrode configuration including an *in-situ* solid silver wire would confirm measurements. Silver wire was embedded adjacent to reinforcement steel inside concrete. A glass tube was also embedded in the concrete in such a way as to provide access near the silver wire and reinforcement steel for a standard Ag/AgCl REF electrode, Fig. 4.4a-b. This way comparison between OCP measurements using the silver wire and OCP measurements using a commercial Ag/AgCl electrode could be made, Fig. 4.5.

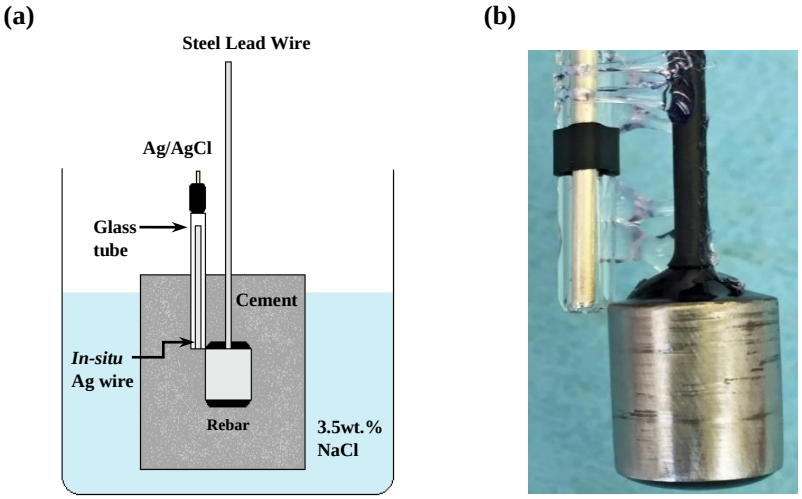

Fig. 4.4 (a) Cross sectional schematic of electrochemical cell for in-situ silver REF electrode studies. The *in-situ* silver wire is outside the glass tube but directly next to it. **(b)** Up close image of silver wire outside the glass tubing and in direct proximity to rebar cylinder.

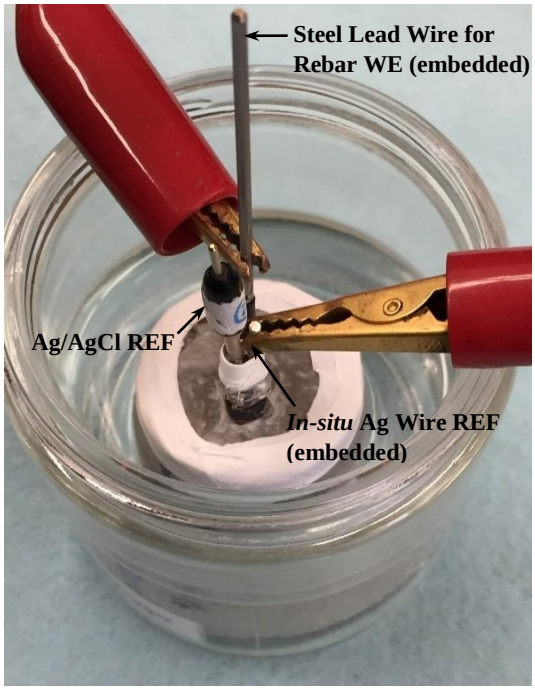

Fig. 4.5 Electrochemical cell, *in-situ* Ag wire as REF, Ag/AgCl as second reference and rebar cylinder WE.

After curing 28 days, concrete cylinders with embedded steel samples were ready for transfer to jars for salt water exposure treatments. After preparation and transfer into 3.5 wt.% NaCl solution, the solution pH before and after immersion of concrete cylinders was measured. After waiting for 24hrs minimum the reference electrode could be inserted into the glass port. Mo-wire coiled around the concrete cylinders would serve as the counter electrode. Each of these, rebar as working electrode, Mo wire as counter electrode and Ag/AgCl as the reference electrode are all connected to the electrometer of the potentiostat (EG&G PAR Model 273A) for corrosion studies. The experiments were run in predetermined time intervals, such as 30, 90, 180 days, etc. Electrochemical techniques included open circuit potential monitoring of the corrosion potential, Linear and Tafel Polarizations to determine corrosion resistance and Cyclic Polarization to characterize chloride induced pitting.

4.2.2 Concrete blocks

This direct measurement technique followed NT Build 443[21] standards and involved extended ponding of cement in salt water followed by incremental analysis of chloride concentration by depth. Glycerol admixture effect on chloride incursion was of interest, admixtures included glycerol at 0.5, 1.0 and 2.0 wt.% vs. cement binder. The admixture was added to the concrete during the mixing process. For a single control block, 600g cement + 600g LnMt sand + 240ml RO H_2O was

used. The standard procedure first mixed cement and sand together as a dry mixture, using a metal stirring whisk. Then glycerol solution was progressively added until concrete was at optimum casting consistency. The Concrete paste was scooped into cube molds and packed down with a plastic rod, concrete block sizes were 8.5 x 8.5 x 8.5 [cm]. Each concrete block was cured for 28 days in a humid atmosphere before ponding began. Ponding was carried out in plastic containers in which blocks were fully submerged by 3.5 wt.% NaCl salt water, Fig. 4.6a-b. Before immersion each block was carefully placed on top of zirconia beads. The beads lift the base surface of the blocks off the bottom of the container. Raising the blocks allowed diffusion of solution through all six faces of each block. Note the images, Fig 4.6a-b, were taken of more recent samples (cylinder shaped) that have yet to finish ponding, however the setup is fundamentally the same.

(a) **(b)**

Fig. 4.6 (a) Sealable plastic container partially filled with simulated sea water. Concrete cylinders within are fully immersed. **(b)** Concrete resting on zirconia beads.

After a ponding period of approximately 1.5 years (550 days), the blocks were removed. Chloride gradient within the concrete was measured by progressive drill sampling from the top, bottom and/or sides of the concrete blocks, Fig. 4.7a-b. The chloride concentration profile was found by analyzing powdered concrete taken at different drill depths. 1.0 gram of concrete powder gathered from each particular drilling depth was suspended in separate 100 ml DI H_2O jars. Following this dissolution, the solutions were left overnight to allow the cement particles to settle down upon which 3mlwas withdrawn from each jar by syringe and filtered through a 0.45 micron PTFE disk filter under syringe pressure. These solutions were analyzed for Cl^- presence using a DioneX Advanced Chromatography Module (IC).

(a) **(b)**

Fig. 4.7 (a) Diamond studded drill (Ø ½'' DAMO) **(b)** Drilling into the top of a concrete block using a drill press, process carried out over a plastic tray.

CHAPTER 5

EXPERIMENTAL RESULTS AND DISCUSSION

5.1 Results

5.1.1 Open circuit potentials

The passive stability of reinforcement steel is dependent on concentrations of both metal ions and electrochemically active species like chloride within the metal and electrolyte (pore solution) interface [15]. Slowing permeation of corrosive species will have an overall effect on corrosion potentials and corrosion current density for the rebar embedded within the concrete matrix. Therefore, periodic electrochemical measurements including open circuit potential (OCP), Linear and Tafel Polarization, and Cyclic Polarization (CP) on the steel can indicate the extent of corrosion. The extent of corrosion reflects the degree of permeability of concrete to chloride containing moisture.

Additionally, metallic silver has been shown to maintain a stable potential in high pH environments [13], due to the formation of an Ag/Ag_2O layer. In alkaline solutions above pH 11, the open circuit potential of silver was unwavering regardless of increases in chloride or oxygen concentrations. Therefore, as previously mentioned, solid silver wire electrodes were studied as *in-situ* reference electrodes embedded in concrete in close proximity to the reinforcing steel. In this way, electrochemical changes to the steel can be measured without risking the structural integrity of the cement. The *in-situ* silver wires also serve to verify the effectiveness of commercially available leak free electrodes which could be susceptible to mineral crystallization plugging from prolonged exposure to concrete pore solution.

For 250 days (36 weeks) all potential changes in the reinforcement steel as specified by the Ag/AgCl REF are attained in kind by the *in-situ* silver wires, Fig. 5.1a-b. The potential difference between *in-situ* solid silver and silver-silver chloride was ~ +0.150 V.

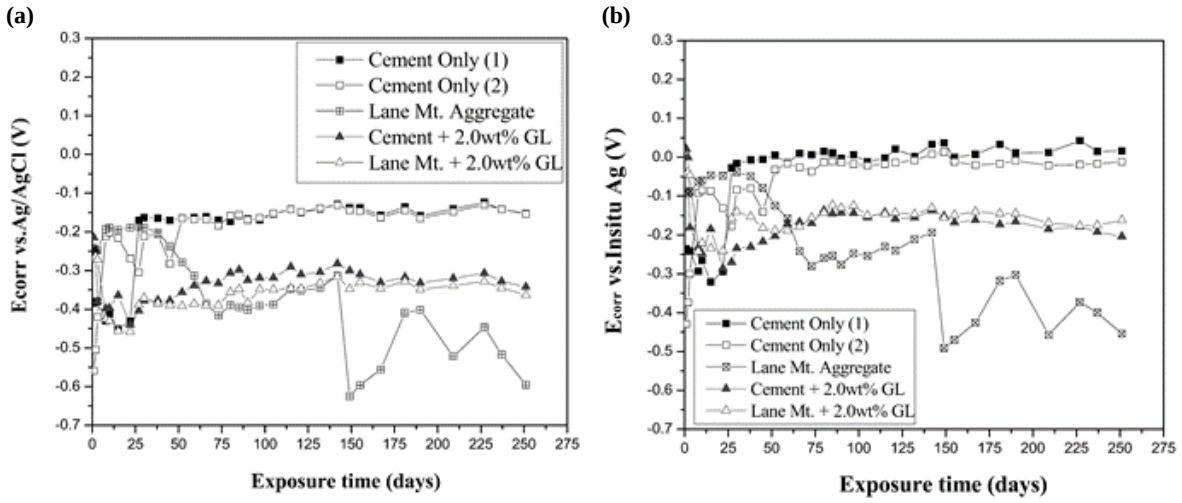

Fig. 5.1 (a) Open circuit potential of rebar working electrode embedded in concrete. Rebar measured against Ag/AgCl REF. **(b)** Open circuit potential of rebar working electrode embedded in concrete. Rebar measured against *in-situ* silver wires.

The OCP for rebar in control samples (Cement Only (1) and (2)) was stable at -0.160 V vs. Ag/AgCl for the entire duration of the experiment. For the cement cylinder containing glycerol admixture 2.0 wt.% (Cement + Glycerol 2.0 wt.%) rebar potential was initially at -0.200 V but moved to a more cathodic potential of -0.350 V where it stabilized. This behavior was mimicked by steel embedded in Lane Mountain aggregated concrete with 2.0wt% glycerol admixture (LnMt + Glycerol 2.0 wt.%). The remaining rebar sample in concrete with Lane Mountain aggregate alone (Lane Mt. Aggregate), showed a stable potential of -0.350 V vs. Ag/AgCl up to 140 days at which time there is an aggressive drop to -0.600 V and then fluctuations of ± 0.150 V over the remaining 100 days.

Prior to the silver electrode experimentation, seven separate concrete cylinders with embedded steel reinforcement were made for CP testing at respective time frames of 1 week, 1 month,1/2 year, and 1 year, see section 5.1.3. Given the extended time period of the later samples, there was an opportunity for additional OCP monitoring.

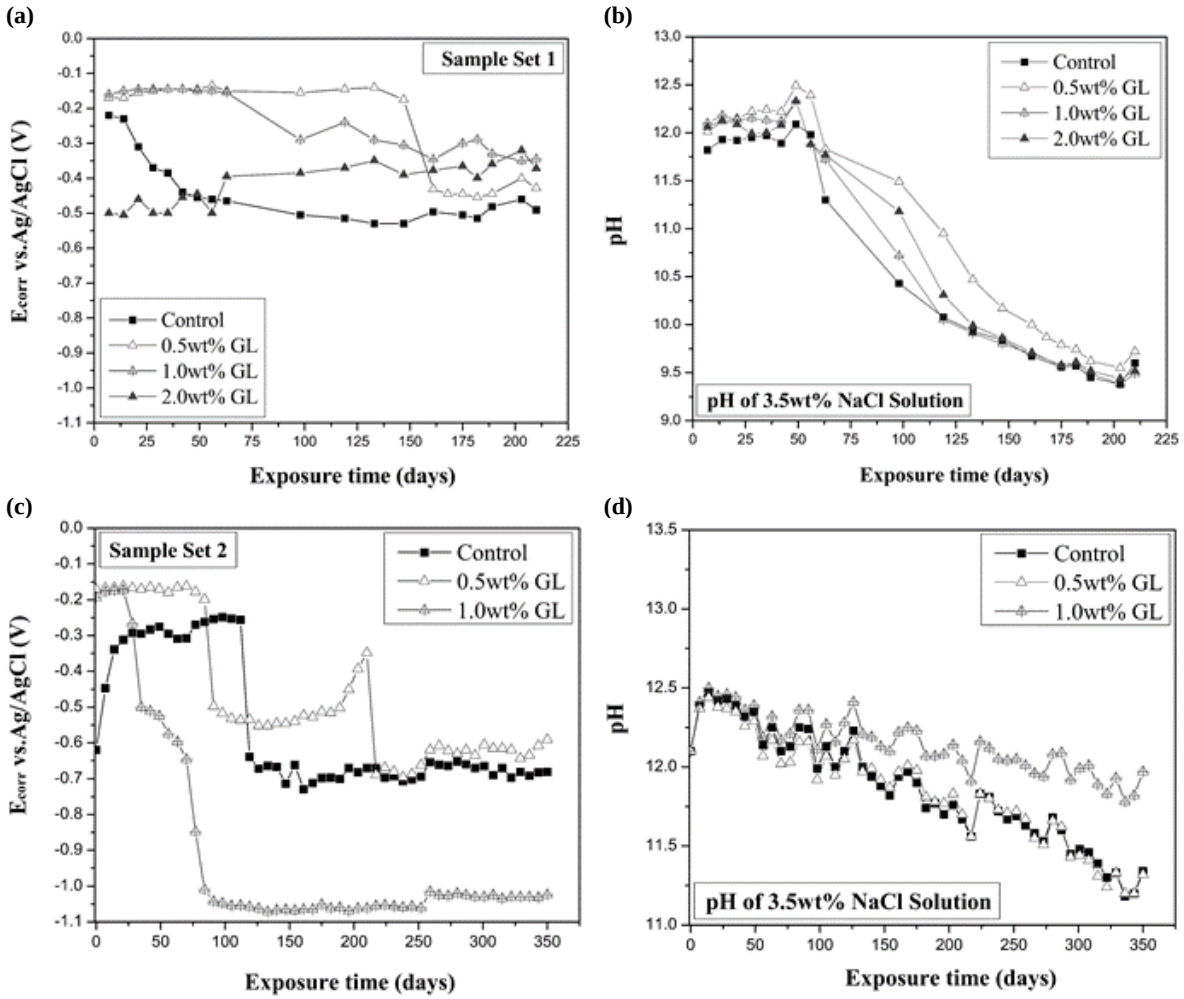

Fig. 5.2 (a) Sample set 1OCPvs. time for rebar embedded in concrete containing glycerol additions of 0.5, 1.0 and 2.0 wt.%. **(b)** pH vs. time for immersion solution (3.5 wt.% NaCl). **(c)** Sample set 2OCPvs. time for replicate rebar samples embedded in concrete containing glycerol additions of 0.5 and 1.0 wt.%. **(d)** pH vs. time for immersion solution containing replicate concrete cylinders.

For the given time intervals (above) concrete samples containing glycerol eventually stabilize at more anodic corrosion potentials then the control experiments (no admixture), with one exception seen in Fig. 5.2c. In Fig. 5.2a, drops in rebar OCP for control, glycerol 0.5 wt.% and glycerol 1.0 wt.% samples are likely caused by chloride anion arrival to the electrode surface. This theory is supported by results from similar OCP measurements done on rebar in direct contact with saturated cement solutions, where chloride was added directly to solution followed by a drop in electrode potential. The open circuit potentials for rebar encased in concrete with glycerol 2.0 wt.%, start low and trend upwards instead of downwards. Starting at an open circuit potential of -0.5V, suggests that at a concentration of glycerol 2.0 wt.%, there was no inhibition of Cl^- migration through the concrete.

However, as time progresses the potential moves more anodic. This could indicate either a slowing of Cl^- arrival, the development of a passive film, or perhaps the formation of glycerol chloride complexes. Further research is needed to identify glycerol's role in the C-S-H chemistry of concrete.

The pH of 3.5 wt.% NaCl immersion solution was monitored in tandem with open circuit potential. The results vary in a range between pH 12.5 and 9.5. The drop in pH occurred marginally slower for salt solution immersing concrete with glycerol added vs. salt solution immersing the control concrete. The drop in pH seen in Fig. 5.2b is credited to the formation of carbonic acid due to carbon dioxide arriving from the air.

Fig. 5.2c displays OCP for a replicate series (Sample Set 2) of rebar samples. For 4 weeks, reinforcing steel in concrete modulated by 0.5 and 1.0 wt.% glycerol remains fixed at -0.160 V vs. Ag/AgCl. Yet, at 5 weeks the reinforcing steel in concrete with 1.0 wt.% glycerol begins to drop "rapidly" before re-stabilizing at -1.5 V vs. Ag/AgCl. The steel embedded in concrete with the 0.5% glycerol admixture exhibits a stable potential for almost 15 weeks, at which point the potential moves negatively to -0.520 V vs. Ag/AgCl where it re-stabilizes for an additional 12 weeks. After the 12-weekinterval, the potential begins to return towards more positive potentials before again dropping cathodically at 30 weeks' time, and was then stable at -0.65 V vs. Ag/AgCl for the remaining 20 weeks of measurements. This is a promising result because the rebar maintains a stable positive potential longer when 0.5wt% glycerol was added to the concrete. A stable positive potential corresponds with rebar steel being less likely to corrode while more negative potentials mean corrosion is more likely to occur. The steel embedded in control concrete (no glycerol) initially started at a potential of -0.60 V vs. Ag/AgCl before progressing anodically to -0.250 V. However, after 15 weeks the potential drops aggressively to -0.700 V vs. Ag/AgCl. In

Again, solution pH surrounding each concrete cell was measured periodically throughout the experiment, Fig. 5.2d. The solution pH does not reflect perfectly the internal pH of the concrete but provides a point of reference. Over 50 weeks, carbonation effect becomes noticeable. From 0-50 weeks the bulk of the samples decreased from an average of pH 12.5 to an average pH 11.25. However, solution ponding the concrete cell with glycerol content at 1.0 wt.% exhibits a much more gradual decline, pH was only reduced to pH 12.0 for this solution. It could be possible that increased viscosity caused by glycerol slows the carbonation reactions kinetics or reacts with the CO_2 itself.

5.1.2 Linear and Tafel polarization

Linear and Tafel polarizations functionalized degree of rebar corrosion per percentage of glycerol admixture cell and exposure time to 3.5 wt.% NaCl solution. Tafel tests scanned at a rate of 0.1667mV/s over a potential range ± 250mV from OCP, and were performed after 7, 30 and 100 days respectively. Before each Tafel polarization an LP would be run. LP tests were run at the same scan rate as Tafel. Application of the Stern and Geary equation was utilized to solve for polarization resistance R_p, depending on experimentally determined values of i_{corr}, β_a and β_c. Tafel polarizations results are shown in Fig 5.3a-d. Electrochemical interpretation of the Tafel tests are tabulated after, Tables 5.1-5.4. The table columns showing the most important values have been shaded.

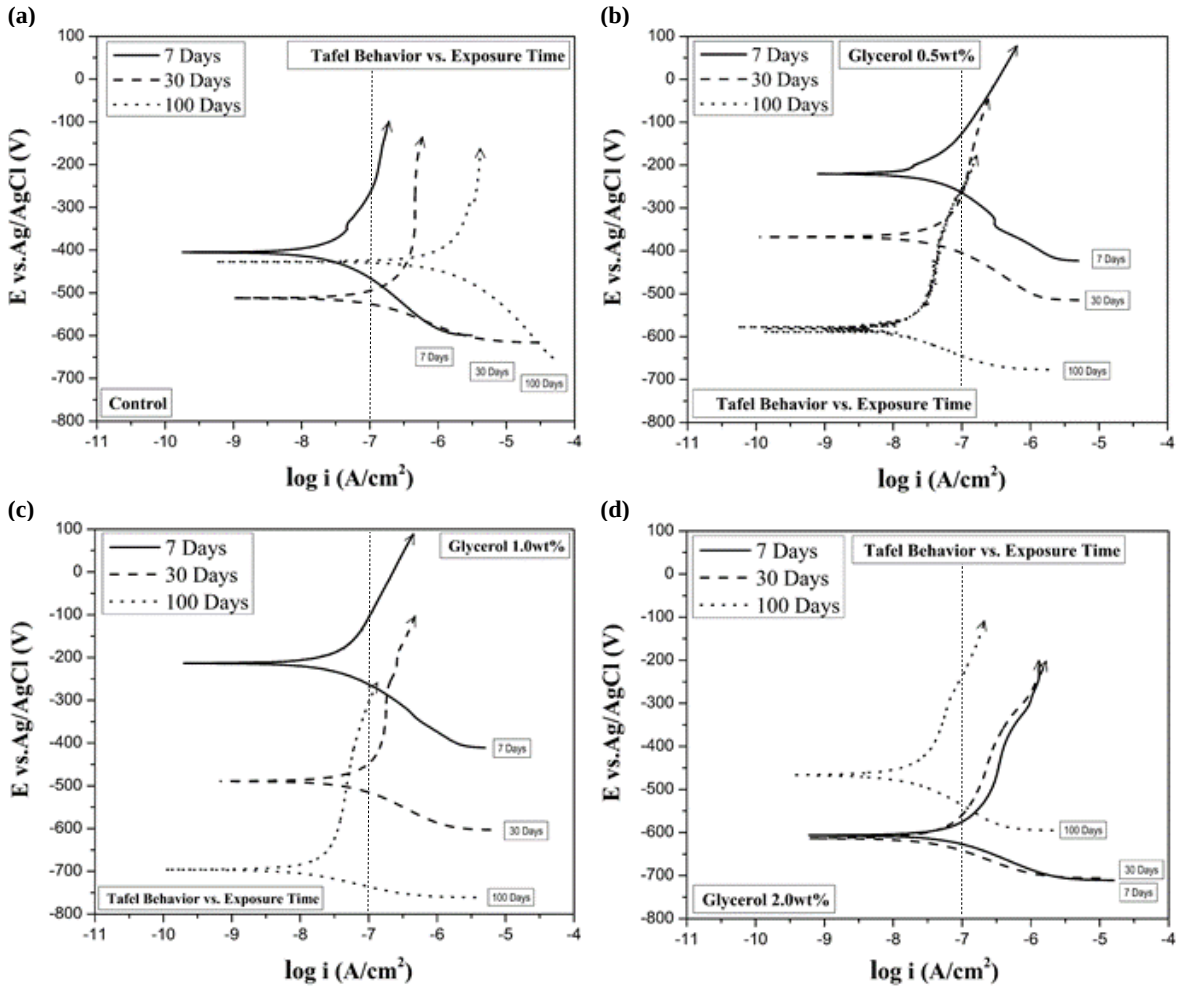

Fig. 5.3 Tafel polarization of rebar embedded in concrete **(a)** without glycerol (control) and with **(b)** 0.5 wt.% glycerol **(c)** 1.0 wt.% glycerol and **(d)** 2.0 wt.% glycerol. Tests were run after concrete had been immersed in simulated sea water (NaCl 3.5 wt.%) for 7, 30 and 100 days. Dashed lines for referencing current density change over time.

Curve location changed for rebar steel in control (no glycerol) concrete at 7, 30 and 100 days. The intersection between anodic and cathodic regions of is near 10^{-8} (A/cm^2) value of current density at 7 days of exposure but moves to the right in increasing order of magnitude with time. At 30 days the polarization curve for the control sample is between 10^{-7} - 10^{-6}(A/cm^2) and at 100 days the intersection point is between 10^{-6} - 10^{-5}(A/cm^2). Interestingly, Tafel curves for rebar in concrete containing any percentage of glycerol do not shift much in current density magnitude over 100 days of exposure time. In fact, observation of Figures 5.3b-d revels that current density decreases over time for rebar embedded in concrete containing any percentage of glycerol. This suggest that glycerol restricts the corrosion rate over time.

Table 5.1 Electrochemical values for Tafel polarization of rebar embedded in *control* concrete, immersed in 3.5 wt.% NaCl for 7, 30 and 100 days.

Exposure (days)	OCP (mV)	E_{corr} (mV)	I_{corr} ($\mu A/cm^2$)	R_p ($K\Omega \cdot cm^2$)	β_a (mV/decade)	β_c (mV/decade)
7	-355.0	-408.8	0.1577	204.54	169.6	132.3
30	-370.00	-513.58	0.094	106.75	36.92	62.38
108	-405.00	-436.48	2.377	14.63	115.3	163.5

Table 5.2 Electrochemical values for Tafel polarization of rebar embedded in *glycerol 0.5 wt.%* concrete, immersed in 3.5 wt.% NaCl for 7, 30 and 100 days.

Exposure (days)	OCP (mV)	E_{corr} (mV)	I_{corr} ($\mu A/cm^2$)	R_p ($K\Omega \cdot cm^2$)	β_a (mV/decade)	β_c (mV/decade)
7	-175.0	-233.6	0.0416	827.24	259.8	114.0
30	-270.00	-377.20	0.0659	287.28	75.76	103.3
108	-430.00	-584.8	0.07508	367.244	469.6	73.45

Table 5.3 Electrochemical values for Tafel polarization of rebar embedded in *glycerol 1.0 wt.%* concrete, immersed in 3.5 wt.% NaCl for 7, 30 and 100 days.

Exposure (days)	OCP (mV)	E_{corr} (mV)	I_{corr} ($\mu A/cm^2$)	R_p ($K\Omega \cdot cm^2$)	β_a (mV/decade)	β_c (mV/decade)
7	-165.0	-216.1	0.04300	840.45	299.9	115.2
30	-360.00	-490.18	0.0544	232.14	46.76	76.93
103	-515.00	-698.36	0.0082	412.51	10.11	33.99

Table 5.4 Electrochemical values for Tafel polarization of rebar embedded in *glycerol 2.0 wt.%* concrete, immersed in 3.5 wt.% NaCl for 7, 30 and 100 days.

Exposure (days)	OCP (mV)	E_{corr} (mV)	I_{corr} ($\mu A/cm^2$)	R_p ($K\Omega \cdot cm^2$)	β_a (mV/decade)	β_c (mV/decade)
7	-465.0	-610.6	0.0658	134.03	29.87	63.55
30	-460.00	-615.92	0.0316	214.61	22.11	53.48
110	-350.00	-467.16	0.0171	851.93	53.59	89.73

At the 7 day testing time the rebar embedded in concrete with 0.5% and 1.0 wt.% glycerol admixtures have nearly identical electrochemical data. Both steels have lower corrosion current densities and higher polarization resistance then the steel embedded in control concrete or concrete with 2.0 wt.% glycerol. The steel with the 2.0 wt.% glycerol modulated concrete actually shows lower corrosion resistance then the steel in concrete without glycerol.

After one month of exposure there is a noticeable decrease in polarization resistance. In steel within 0.5, 1.0 and 2.0 wt.% glycerol modified concrete polarization resistance stabilized to approximately 250 $K\Omega \cdot cm^2$. The control sample steel decreased in polarization resistance to the lowest value out of the four samples. The polarization resistance for steel in the 2.0 wt.% sample increased slightly compared to the 7 day test.

After 100 days exposure time, steel polarization resistance is highest in concrete with glycerol admixtures and increases with percentage of glycerol. The steel in control concrete has higher current density by several orders of magnitude and the lowest resistance to polarization.

The linear polarization results at 30 and 100 day test times are given below, Table 5.4-5.5.In many cases there was no recognizable linear region. When no linear region was present a tangent linear fit was used over a ±10 mV range about OCP.

Table 5.5 Resistance values from linear polarization of rebar embedded in concrete immersed in 3.5 wt.% NaCl solution for 30 days.

Admixture (wt.%)	Exposure (days)	OCP (V)	Rp (KΩ)
Control	30	-0.178	4910
Glycerol 0.5%	30	-0.330	1520
Glycerol 1.0%	30	-0.448	606

Table 5.6 Resistance values from linear polarization of rebar embedded in concrete immersed in 3.5wt% NaCl solution for 90 days.

Admixture (wt.%)	Exposure (days)	OCP (V)	Rp (KΩ)
Control	100	-0.729	595
Glycerol 0.5%	100	-0.541	466
Glycerol 1.0%	100	-0.523	432

The results for linear polarization were inconclusive. If anything, polarization resistance decreases with increasing glycerol concentration, this contrasts with Tafel measurements. Difficulty in LP measurements for steel embedded in concrete could result from the high pH environment. The large number of hydroxides present in concrete could be forming an OH^- barrier on the rebar, interfering with sensitive LP measurements making the results difficult to interpret.

5.1.3 Cyclic polarization

Localized pitting corrosion can be measured using the electrochemical method of cyclic polarization. This method is potentio-dynamic like Tafel, but scans along a much higher anodic range. Forward scans were initiated at -250mV vs. OCP then allowed to continue to a noticeable break in passive behavior characterized by a rapid increase in current density with increasing potential, this is the transpassive region. At this point, the scans were reversed and the nature of the hysteresis observed. If the scan returned left and traced back along the transpassive region then this hysteresis was negative and represented no pitting. In contrast upon reversal of the scan direction if the return was to the right with no reduction in current density with decreasing potential then the scan had a positive hysteresis and represented localized corrosion attack.

CP tests were conducted to observe admixture effect on chloride initiated pitting for rebar embedded in concrete. If glycerol additives restrict the arrival of chloride ions, corresponding decreases in pitting currents and increases in passive potentials would be observed.

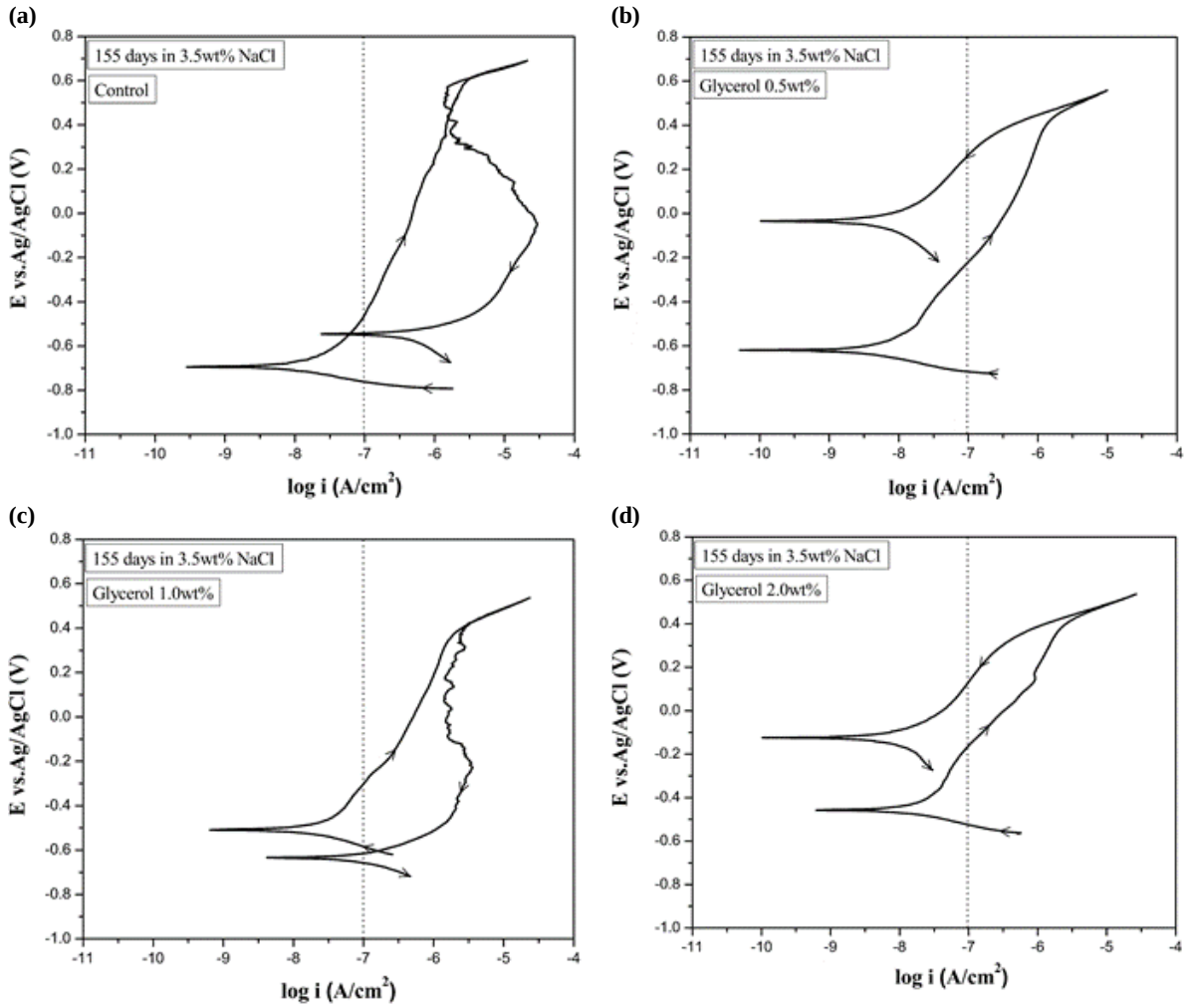

Fig. 5.4 Cyclic polarization of Rebar embedded in concrete with**(a)** no glycerol admixture**(b)** glycerol 0.5wt% **(c)** glycerol 1.0wt% and **(d)** glycerol 2.0wt%. Experiments run after concrete had been immersed in simulated sea water (NaCl 3.5wt %) for 155 days.

Fig. 5.4a-d are resulting cyclic polarization graphs for the first series of rebar electrodes cast in concrete. This was the same series of electrodes used for OCP monitoring, Fig. 5.1a. After 5 months immersed in salt water, the CP for rebar embedded in concrete without glycerol addition (control), exhibits a positive hysteresis, Fig. 5.4a. The positive hysteresis indicates pit formation on the rebar surface. For rebar embedded in concrete with the glycerol additions, CP analysis indicates no pitting present at glycerol concentrations of 0.5 and 2.0 wt.%. Conversely, the glycerol 1.0 wt.% admixture concrete has pitting present on the rebar surface. Furthermore, current density amplitude (dashed line for reference) is the same for the glycerol 1.0 wt.% parameter as for the control CP. To contest the results of this first series of tests a second round of cyclic polarizations was performed, Fig. 5.5a-c. Immersion times in salt water before cyclic polarization were 30, 90 and 350 days.

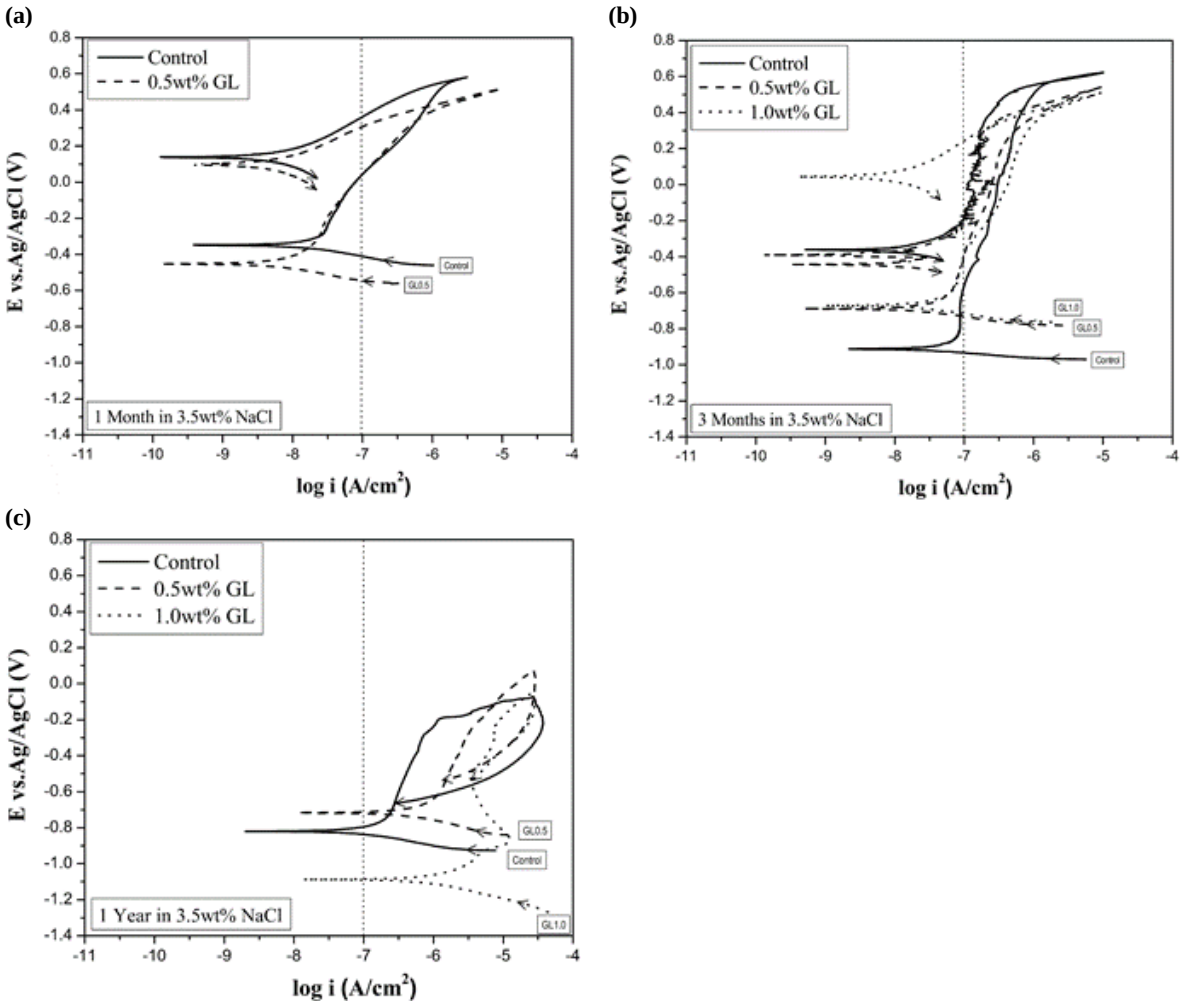

Fig. 5.5 Cyclic polarization curves for rebar in concrete with and without glycerol admixture. Cyclic polarizations run after **(a)** 1 month (30 days) **(b)** 3 months (90 days) and **(c)** 1 year (350 days) of exposure to 3.5wt% NaCl solution.

Fig. 5.5a represents potentiodynamic scans on embedded rebar after 30 days of concrete exposure to salt water. Both scans are similar, there is little to differentiate between control and glycerol 0.5 wt.%. Both scans have a negative hysteresis but don't exhibit fully passive behavior. Both forward scans have a slight slope, meaning current is still slightly increasing with potential.

The polarization of steels embedded in concrete after three months treatment in saltwater are shown in Fig. 5.5b. In this case, rebar pitting was avoided by all three parameters. The control scan has the greatest passive potential range but the glycerol 1.0 wt.% sample has the fastest repair. The repair (re-passivation) potential is identified at the transition from anodic to cathodic (Tafel region) behavior on the return scan.

Fig. 5.5c displays the longest exposure time of 1 year before CP runs. The final three CPs all show pitting, however the extent of the pitting determined by the size of the hysteresis loop is much

smaller for the rebar in concrete which had glycerol admixtures present. Furthermore, the repair potentials (where the return scan intersects the forward scan) are higher for steels in both glycerol 1.0 and 0.5 wt.% modified concrete than control. However, current densities for rebar in all glycerol modulated concrete were slightly higher than control and rebar in the glycerol 1.0 wt.% concrete cylinder exhibited a passivation behavior not seen in the other two scans.

5.1.4 Chloride Concentration Gradients

Drilling directions into the concrete blocks included top-down, side-in and base-up. For example, the chloride concentrations with depth have been presented, Fig. 5.6a-e.

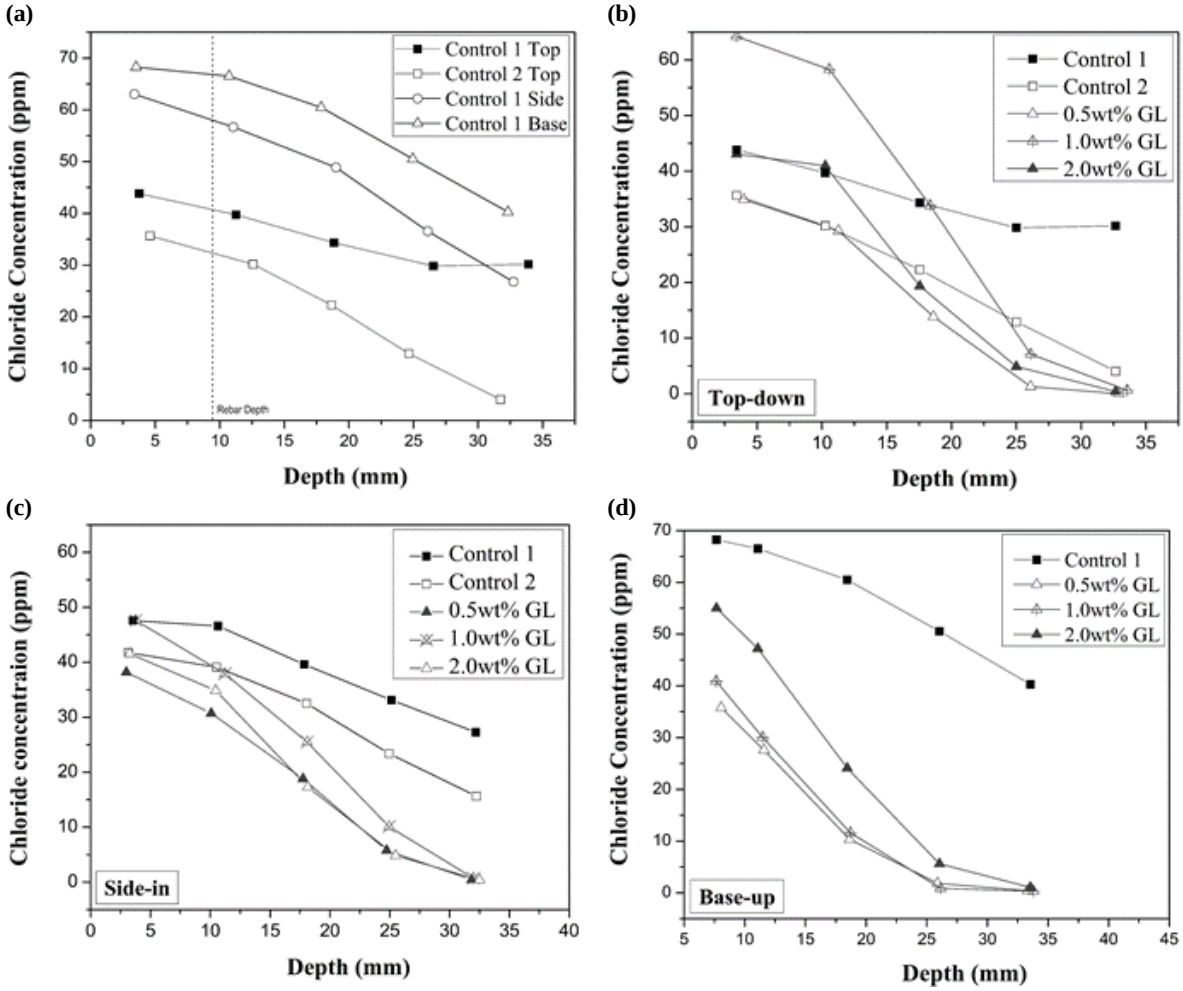

Fig. 5.6 Chloride concentration profiles for concrete **(a)** control samples, **(b)** glycerol admixtures profiles from top-down direction of drilling, **(c)** glycerol admixtures profiles from side-in direction of drilling, **(d)** glycerol admixtures profiles from base-up direction of drilling.

There is a disparity in chloride profiles dependent upon drilling direction. There were six faces on each of the blocks and two planes of drilling, vertically (top-down or base-up) and horizontally (side-in). A considerable degree of difference was found between chloride concentrations for top-down and base up. One explanation for this is gradation in concrete density. During concrete casting stage, the cement aggregate paste is subject to gravitational effects and separation. The denser and heavier aggregates will tend to descend in the mold and sedimentate at the bottom while free water will rise to the top. This is true in the cement phase as well, less dense fluid will be pushed upwards as cement particles compact and settle downwards. This process will create a solid concrete sample with a slightly denser base and less dense top surface. Precautions to prevent this were taken during sample preparation. Preparation included progressive compaction and manual vibration of each sample, even so not 100% of the separation can be prevented. Furthermore, due to evaporation, there was an interval of several weeks, in which the salt solution level dropped below the tops of the blocks. Sodium chloride does not evaporate with water but remains behind in solution. Therefore in order to not change the salt concentration DI water was used to bring the solution level back to its original volume.

Fig. 5.6a. Illustrates the variance in chloride concentration profiles dependent upon the drilling direction. The top down direction shows lower chloride concentrations of chloride for the initial 25mm. Note two separate control blocks were made for confirmation purposes. There is a marked difference in the concentration profiles from control 1 to control 2. The slope is gradual in control 1 for the top down drill direction while the slope of control 2 is much steeper. However, examination of Fig. 5.6c shows that the side-in direction of drilling had control samples profiles more tightly grouped. The highest concentrations of chloride in control concrete were seen in the base-up drilling direction with the side in drilling direction slightly less. The dashed line in Fig. 5.6a marks the depth at which rebar electrodes were embedded during the electrochemical studies.

It can be seen in Fig. 5.6b-d, that glycerol increases the slope (concentration gradient) of the lines, indicating a greater decrease in chloride presence moving towards the center of the blocks. Furthermore, in blocks containing glycerol, chloride concentration values are at and below 1ppm near the center of the block. The lowest chloride concentrations were seen in the block with 0.5 wt.% glycerol. It could be at higher concentrations of 1.0 and 2.0 wt.%, the glycerol slightly inhibits the C-S-H chemistry and prevents formation of a denser microstructure. Regardless at any concentration of glycerol the chloride profiles are much steeper than the controls.

By application of Crank's solution to Fick's 2nd law, the diffusion coefficients *D* as a function of glycerol admixture were calculated. [22]

$$\frac{C_x - C_o}{C_s - C_o} = 1 - erf\left[\frac{x}{2\sqrt{Dt}}\right] \quad (4)$$

Here C_x is the concentration of chloride in ppm at a certain depth x. C_s is the concentration of chloride at the surface of the concrete which was assumed to be 3.5wt% equivalent to 35000 ppm. C_o is the concentration of chloride within the concrete at time 0, this was assumed to be zero, there is a certain amount of bound chloride (0.2ppm) present in the cement before casting but it is assumed to be negligible. The time of exposure is represented by t which for this experiment was t = 550 days. Note calculations were done for the side-in drilling direction alone. The degree of difference between control 1 and 2 was smallest for the side in direction. Additionally, drilling side in-wards negates the error that could arise from evaporation loss (top face exposed to air) and in the middle gradation effects are averaged.

Table 5.7 Effect of glycerol admixture on concrete diffusivity

Admixture (wt.%)	Concentration gradients (ppm/mm)	Diffusion coefficients (cm^2/s)
Control 1	-0.754	$0.97x10^{-8}$
Control 2	-0.935	$0.89x10^{-8}$
Glycerol 0.5%	-1.39	$0.56x10^{-8}$
Glycerol 1.0%	-1.73	$0.59x10^{-8}$
Glycerol 2.0%	-1.53	$0.58x10^{-8}$

The calculated diffusion coefficients are shown in Table 5.7. There is some discrepancy in values between the control samples. The percentage difference between the controls was 8.6%, if the values are averaged the control concrete has diffusivity of $0.93x10^{-8}$ cm^2/s. The greatest percentage difference between glycerol augmented concrete samples was 5.2%, if the values are averaged the glycerol concrete has diffusivity of $0.58x10^{-8}$ cm^2/s. These results show that the factor for chloride diffusivity between concrete with glycerol and concrete without glycerol is 1.6 times smaller for the glycerol modulated concrete.

5.2 Discussion

Chloride ion transport is directly related to water transport by two mechanisms, advection, and diffusion. In advection, capillary forces are the main mechanism of water ingress and dissolved chloride ions are transported along by the liquid. The diffusion process is governed by concentration

gradients and chemical potentials. How glycerol as a viscosity modifier effects these mechanisms will depend on how glycerol interacts with the C-S-H gel.

5.2.1 Glycerol's Role in C-S-H Hydration

The fundamental interaction between glycerol and the porous medium is still uncertain. The key question being, do the hydroxyl groups react in part during C-S-H hydration? If involved in the hydration reactions between calcium oxides, silica and water, the glycerol could be partially or fully bound within the cement matrix. If glycerol is fully bound by the C-S-H gel then it would not be free to affect viscosity of the pore solution. In this case, glycerol would be acting solely as a retarder and slowing hydration reactions. In its own right this can still be useful but not in terms of viscosity modulation of pore solution.

The second possibility is, only one or two of the available hydroxyl groups are bound during hydrations, leaving open ended negatively charged functional groups which stretch into the porous cavities. These portions would affect the pore solution viscosity. This would be ideal, since the bound molecules are rigidly held by the concrete and not subject to diffusion out of the concrete. This is one possible downside to the viscosity modifier, in wet rainy climates, the constant wetting and drying would actively leach out glycerol and in marine/tidal environments this process would only be accelerated. It should also be mentioned that glycerol is hygroscopic. In a wet-dry cycle, glycerol could be detrimental by actively absorbing moisture into the concrete. However if the concrete is fully saturated by moisture the glycerol then becomes beneficial in that the viscosity of the pore solution is increased. Further research is needed to understand glycerol effect on concrete in a wet dry cycle.

The final possibility would be glycerol is left unbounded and the entire molecule is free in the pore solution. If the entirety of the molecule is in solution it would result in the most viscosity adjustment. Secondary conjecture to this would be if molecules of glycerol experience any attractive forces towards the pore walls. These attractive forces could be charge driven or by surface area effect. Zang and Gjorv proposed that an effective electrical double layer of adsorbed ions can form on the walls of the porous cavities. [23] In this case, conglomerating glycerol molecules could effectively form a potential barrier to the similar charged chloride ions.

In addition, Song and Rochelle have shown that glycerol in hydroxide solutions will react to from glyceroxide. [24] In this case, the open-ended chain of one of the functional groups would be a negatively charged oxygen atom. They further presented the possible glyceroxide reaction with CO_2.After the carbonation reaction the glycerol molecule has an additional three oxygen atoms one of

which is still negatively charged. In the concrete system, this could have several beneficial effects. One benefit is that the glycerol consumption of CO_2 would slow the pH reduction in the pore solution providing further protection to the reinforcement steel. This could be one explanation for results seen in Fig. 5.2d. The second benefit, on top of being a larger molecule which enhances viscosity effect, glyceroxide still has a negative charged oxygen atom which would repel Cl^- ions and slow diffusion.

5.2.2 Relating Diffusivity to Viscosity

If glycerol is free in solution then the proposal set forth by Bentz is applicable. The results from experiments on blocks with prolonged ponding in salt solution, show a glycerol effect. Even in the small concentrations of 0.5, 1.0 and 2.0 wt.%, glycerol decreased the diffusivity of chloride by a factor of 1.6. The Bentz equation derived from the Stokes-Einstein relationship relating viscosity and diffusion allows for theoretical deduction of possible viscosity change induced by glycerol admixtures within porous pathways.

$$\frac{D}{D_o} = \frac{\eta_o}{\eta} \qquad (5)$$

Here, D is the diffusion coefficient after and D_o the diffusion coefficient before viscosity change. The diffusion coefficient after is taken to be the average diffusion coefficient from the three glycerol modulated concretes $D = 0.58 \times 10^{-8}$ cm^2/s. The original diffusion coefficient was averaged from the diffusivities of the control concrete $D_o = 0.93 \times 10^{-8}$ cm^2/s. The change in viscosity is represented by the ratio η_o original viscosity and η the new viscosity. The new viscosity of glycerol pore solution is predicted at η = 1.6 mPa•s. A 10% glycerol water solution has a viscosity of only 1.31 times that of just water. [25] The highest concentration of glycerol at 2.0wt% to binder was achieved by adding 1.0 g of glycerol to 20 g water, Table 4.3. This is only a 5% glycerol solution, meaning there must be a concentrating effect of glycerol within the pore pathways. This could result from the C-S-H hydration reactions, in which tricalcium silicate (C_3S) and tricalcium aluminate (C_3A) formation consumes water and leaves behind in full or in part the glycerol. When the pore cavities receive moisture from capillary action the glycerol concentration is now much higher due to the small pore volumes. A viscosity increase to 1.6 mPa•s, assuming an original viscosity of 1.005 mPa•s, would represent a glycerol concentration near 20% within the pore cavities. Another possible explanation for the perceived viscosity increase would be that a component of the diffusivity reduction is related to a potential barrier towards Cl^- ions caused by the hydroxyl groups of glycerol or negatively charged oxygen in glycerol oxide, as previously mentioned.

5.2.3 Interpretations from Electrochemical Studies

The principle behind using electrochemistry to measure alterations to diffusivity was, the more chloride and moisture allowed to arrive to the rebar surface the greater the extent and rate of corrosion. By studying electrochemical behavior of reinforcement steel at different time intervals, glycerol effect on diffusion could thereby be inferred. However, determining glycerol effect on diffusivity from the corrosion results is difficult. It has been shown that glycerol can function as a corrosion inhibitor. [26] In pH 12.5 cement saturated solutions (simulates the internal pore solution) glycerol was seen to increase the chloride threshold concentration for pitting to 81 x 10^{-3}mol/L from 50 x 10^{-3}mol/L. Glycerol may play a role in stabilizing the iron oxide film which protects steel from corrosion. Any reductions in current density with time or increases in polarization could be in part due to glycerol inhibition effect at the steel concrete interface and not solely viscosity effect within the pores. Nonetheless the electrochemical results merit further discussion.

5.2.4 Open Circuit Potentials

In general, the more cathodic (negative) an electrode potential the more likely the metal will undergo oxidation. To a degree, a negative charge represents the number of electrons available for reaction. If an electrode has a more anodic (positive) charge it has less probability of undergoing corrosion by oxidation.

The AMST C876-15 standard states that reinforcing steel has a 90% probability of no corrosion when open circuit potentials are more positive than -0.20 V vs. CSE ($Cu/CuSO_4$). [27] If rebar potential is between -0.20 and -0.35 V vs. CSE corrosion activity in that area is uncertain. If rebar potential is below -0.35 V vs. CSE there is a 90% probability of corrosion. Taking into account the difference between copper-sulfate (0.318 V) and silver chloride (0.222 V) reduction potentials, means rebar will have a 90% probability of no corrosion at OCP more positive than -0.104 V vs. Ag/AgCl. Rebar corrosion will be uncertain at open circuit potentials between -0.104 and -0.254 V vs. Ag/AgCl and rebar corrosion is 90% probable at potentials more negative than -0.253 V vs. Ag/AgCl. In a highly alkaline solution, research supports that at the surface of solid silver a mono-layer of Ag-OH will form followed by a secondary reaction to form Ag_2O. [28] [29] It is believed that the *in-situ* silver wires embedded as reference electrodes, have a layer of Ag_2O which is sustained by the high concentrations of hydroxide. If there is any disruption in the silver oxide layer caused by chloride it can be immediately repaired. In this way the silver wires are held at constant potential not influenced by the potential of the pore solution. However this stability is dependent upon pH. Studies have shown

that other metal/metal oxides embedded in concrete have a stability dependent upon pH [30] [31] [32]. The solid silver wires will be effective reference electrodes until carbonation sufficiently lowers pH.

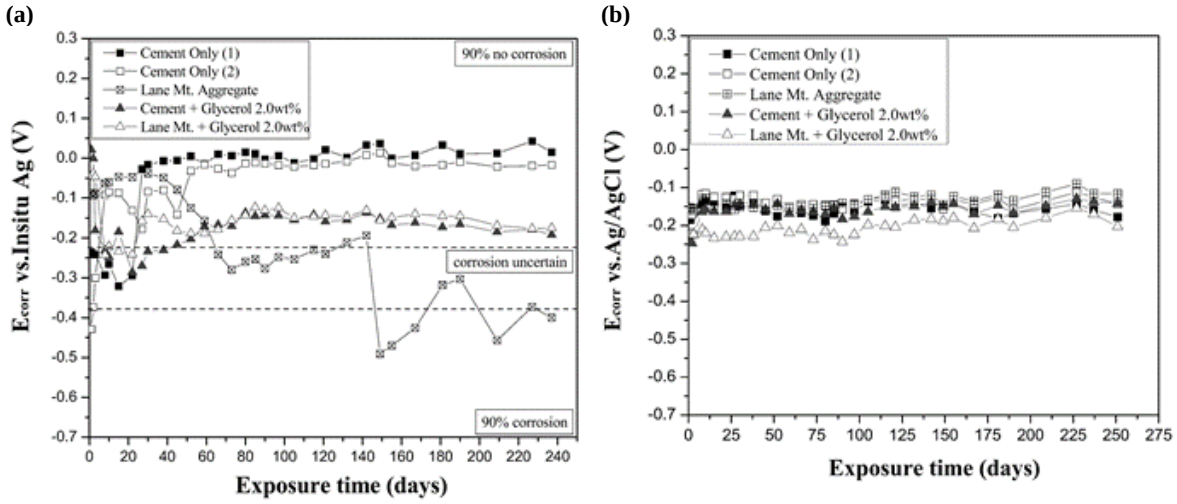

Fig. 5.7 (a) Open circuit potential of rebar embedded in concrete measured against *in-situ* silver wires. Dashed lines represent boundary regions for low, uncertain and high probability of corrosion. **(b)** Open circuit potential of silver wire (Ag_2O) embedded in concrete measured against Ag/AgCl standard reference.

The reduction potential difference between silver chloride (0.222V) and silver oxide (0.342) is 0.120V. Therefore, at potentials more positive than -0.224 V vs. Ag_2O there is a 90% probability that no corrosion is occurring on the rebar surface. At potentials between -0.224 and -0.374 V vs. Ag_2O corrosion probability is uncertain for rebar. At potentials, more negative than -0.374 V vs Ag_2O probability of rebar corrosion is 90%. Using these standards, and observations from Fig. 5.1b, regions of corrosion and non-corrosion can be shown, Fig. 5.7a. Both control cement parameters have rebar potentials in the non-active corrosion region. The concrete and cement with glycerol 2.0 wt.% admixture both have steel potentials nearing but still above the grey area of corrosion uncertainty. It is speculated that glycerol admixture affects the rest potential of rebar steel. The additional hydroxide groups from glycerol could be the reason potentials are 100mV more cathodic for rebar in glycerol modified cement or concrete vs. cement or concrete alone. Normally, more cathodic potentials mean more electrons available for oxidation. But the rebar in the cement or Lane Mt aggregate concrete with glycerol 2.0 wt.%, most likely receives defense from corrosion by glycerol slowing incursion of moisture while also providing inhibiting effects against corrosion, thus negating the effects of having a lower potential.

The final sample of rebar in the Lane Mountain aggregated concrete (without glycerol) is in the active corrosion region. One explanation for this sample being in the active corrosion region, while the cement only samples are not, depends upon the aggregate. Cement only samples have 100g of

cement used in each casting while the Lane Mt sample has 50 g cement and 50g sand. By volume, the cement only samples will have greater concentrations of hydroxides which play a role in formation of the iron oxide passive film. Extra hydroxide concentration means more robust resistance to corrosion resulting from carbonation processes. Furthermore, silica aggregate itself has wetting properties which may aid moisture uptake. Add to this, the extra space between C-S-H gel and silica aggregate grain boundary, which increases overall permeability.

To continue the discussion concerning OCP, Fig 5.2a and Fig. 5.2c shows results of OCP monitoring prior to CP analysis. By the end of these experiments, all rebar samples were in the 90% probability of corrosion region. Additionally, the second set of samples had one reinforcement steel sample (glycerol 1.0 wt.% parameter), with an abnormally low potential of -1.5 V vs. Ag/AgCl. At this low of a potential the steel is nearly cathodically protected from corrosion. However, polarization analysis revealed pitting on the rebar surface after 1 year exposure to salt solution, Fig. 5.5c. This means, the steel was close to but not entirely cathodically protected. Extent of glycerol influence on the OCP in this sample is still unknown. For both sample sets, series one Fig. 5.1a and series two Fig. 5.1c, the reinforcement steel in glycerol 0.5wt.% concrete maintained the highest potentials for the longest times.

5.2.5 Polarizations Methods

The follow up CP experiments showed E_{corr} potential decreasing with time across all sampling parameters. Note, due to the destructive nature of cyclic polarization, separate sample sets had to be made for each scheduled testing time. One set was tested at one week, another set was tested after a month and so on. This was also the case for Tafel analysis.

Overall, in terms of Tafel and CP tests, the rebar steel in glycerol 0.5 and 1.0 wt.% concrete showed the most consistent resistance to corrosion. Implying a reduction in chloride diffusion or a corrosion inhibition or a combination of both. This is identified in Tables 5.3-5.5 from Tafel as well as the nature of the CP graphs. The glycerol 0.5 and 1.0wt.% additions showed higher R_p values for the rebar than the control sample on each testing time (7, 30, or 100 days). For CP, after one week and one month, glycerol modified samples showed lower current densities and more anodic repair potentials for the rebar. Only after one year did steel in concrete with glycerol modifications show higher current densities than control. Even so, the hysteresis loops in this case were less pronounced and repair potentials more positive.

CHAPTER 6

CONCLUSIONS

6.1 Summary

Glycerol as a viscosity modifier was added to both cement and concrete blends during the mixing stage. Objectively glycerol's high viscosity will slow the diffusion of chloride through the concrete pore solution. Furthermore, the glycerol molecule has three functional hydroxyl groups, this raises the alkalinity of the cement paste and could slow the carbonation processes while also inhibiting corrosion. The results of direct drilling measurement as well as indirect electrochemical studies led to the following conclusions.

6.2 Conclusions

1. Rebar cylinders embedded in Lane Mt concrete with 2.0 wt.% glycerol and cement with 2.0 wt.% glycerol exhibited open circuit potentials in the region 90% safe from corrosion for 250 days.
2. Other OCP experiments showed rebar in concrete containing glycerol tended to have more anodic potentials than rebar in concrete without glycerol.
3. Tafel polarization tests over three different time frames revealed that rebar in concrete with glycerol 0.5 and 1.0 wt.% modulation achieved higher resistance to polarization (corrosion) with lower current density than rebar in unmodified concrete.
4. Cyclic polarization tests at 30 days and 90 days indicated slightly higher repair potentials for rebar in glycerol modified concrete.
5. CP runs following half a year and one full year of concrete exposure to 3.5 wt.% NaCl specified rebar having abbreviated hysteresis loops and more anodic repair potentials than rebar in the control concrete.
6. Direct drilling measurements following 550 days of salt water ponding, defined a noticeable reduction in chloride ingress in concrete modified with glycerol. Total reduction to diffusivity was calculated at a factor of 1.6 times.
7. Glycerol restricts moisture and chloride transport through cement/concrete systems at an optimal ratio of 0.5wt% glycerol admixture.

FUTURE WORK

One of the projects key objectives was to reduce permeability of concrete to the chloride ion. Previously discussed was measurement of chloride concentration by depth within concrete blocks. Although the results of concrete block ponding were satisfactory, the duration of the experiment from start to finish was nearly two years. This prolonged ponding was necessary to allow for the slow ingress of chloride through the large concrete blocks.

Thus, a novel approach for accelerated chloride penetration by application of pressure is proposed. To best study the diffusion of Cl^- ion, a series of concrete cylinders will be cast then immersed in salt water and placed in an autoclave. The high pressures attainable inside the autoclave should accelerate the ingress of moisture and chloride into the concrete. The effectiveness of the proposed method will be investigated.

REFERENCES

[1]Gagg, C.R. Cement and Concrete as an Engineering Material: An Historic Appraisal and Case Study Analyses. Eng. Fail. Anal. **2014,** 40, 114-140.

[2]Sanders, M.C.; Sanders C.E. A Worlds Dilemma upon Which the Sun Never Sets -The Nuclear Waste Management Strategy (Part 1): Western European Nation States and the United States of America. Prog. Nucl. Energy. **2016**, 90, 69-97.

[3] Cedolin, L.; Poli, S.; Iori, I, Tensile Behavior of Concrete. J. Eng. Mech. **1987**, 113(3), 431-449.

[4] Cheng, S.; Shui, Z.; Li, Q.; Sun, T.; Yang, R. Properties, Microstructures and Hydration Products of Lightweight Aggregate Concrete with Metakaolin and Slag Addition. Const. Build. Mater. **2016**, 127, 59-67.

[5] Fajardo, G.; Valdez, P.; Pacheco, J. Corrosion of Steel Rebar Embedded in Natural Pozzolan Based Mortars Exposed to Chlorides. Const. Build. Mater.**2009**, 23, 768-774.

[6] Bentz, D.P.; Snyder, K.A.; Cass, L.C.; Peltz, M.A. Doubling the Service Life of Concrete Structures. I: Reducing Ion Mobility Using Nanoscale Viscosity Modifiers. Cem. and Concr. Compos. **2008**, 30, 674-678.

[7] Bentz, D.P.; Snyder, K.A.; Peltz, M.A. Doubling the Service Life of Concrete Structures. II: Performance of Nanoscale Viscosity Modifiers in Mortars. Cem. and Concr. Compos. **2010**, 32, 187-193.

[8] Minor, C.S.; Dalton, N.N. Glycerol: Chemical properties and Derivatives of Glycerin. American Chemical Society. **1953**; Monograph 17.

[9] Sullivan, J.A.; Burnham, S. The Use of Alkaline Earth Oxides as pH Modifiers for Selective Glycerol Oxidation Over Supported Au Catalysts. Renewable Energy. **2015**, 78, 89-92.

[10] Cerny R, Rovnanikova P. Transport processes in concrete. Spon Pres, London, **2002**, pp. 2-3.

[11] Jennings, H.M.; Bullard, J.W.; Thomas, J.T.; Andrade, J.E., Chen, J.J.; Scherer, G.W. Characterization and Modeling of Pores and Surfaces in Cement Paste: Correlations to Processing Properties. J. Adv. Concr. Technol. **2008**,6, 5-29.

[12] Rangaraju, P.R.; Olek, J.; Diamond, S. An Investigation into the Influence of Inter Aggregate Spacing and the Extent of the ITZ on Properties of Portland Cement Concretes. Cem. Concr. Res.**2010**, 40, 1601-1608.

[13] Song, G. Equivalent Circuit Model for AC Electrochemical Impedance Spectroscopy of Concrete. Cem. Concr. Res. **2000**, 30, 1723-1730.

[14]Pavlik, Z.; Fiala, L.; Madera, J.; Pavlikova, M.; Cerny, R. Computational Modelling of Coupled Water and Salt Transport in Porous Materials using Diffusion-Advection Model. J. Franklin. Institute. **2011**, 348, 1547-1587.

[15] Jones, D.A. Principles and Prevention of Corrosion, 2nd ed.; Prentice Hall: New Jersey, **1996**.

[16] Pourbaix, M. Atlas of Electrochemical Equilibria in Aqueous Solutions, National Association of Corrosion Engineers: Houston Texas, 1974.

[17] Andrade, C.; Alonso, C. Corrosion Rate Monitoring in the Laboratory and on Sight. Const. Build. Mater. **1995**, 10, 315-328.

[18] Tait W.S. An Introduction to Electrochemical Corrosion Testing for Practicing Engineers and Scientists, PairODocs Publications: Wisconsin, **1994**.

[19] Stern, M.; Geary A.L. Electrochemical Polarization: I. A Theoretical Analysis of the Shape of Polarization Curves, J. Electrochem. Soc. **1957**, 104, 56–63.

[20] AMST C192 192M-06: Standard practice for making and curing concrete test specimens in the laboratory.

[21] NT Build 443: Concrete hardened: accelerated chloride penetration.

[22]Crank J, The mathematics of diffusion, Oxford University Press, **1975**

[23]Zhang, T.; Gjorv, O.E. Diffusion Behavior of Chloride Ions in Concrete. Cem. Concr. Res. **1996,** 26, 907-917.

[24]Song, D.; Rochelle, G.T. Reaction Kinetics of Carbon Dioxide and Hydroxide in Aqueous Glycerol. Chem. Eng. Sci. **2017**, 161, 151-158.

[25]Segur, J.B.; Oberstar H.E. Viscosity of Glycerol and its Aqueous Solutions. Ind. Eng. Chem. **1951**, 43, 2117-2120.

[26]Blair, R.D.; Pesic, B.; Kline, J.; Ehrsam, I.; Raja, K. Threshold Chloride Concentrations and Passivity Breakdown of Rebar Steel in Real Concrete Solution at Different pH Conditions with the Addition of Glycerol. Acta. Metall. Sin. (English Letters). **2017**; DOI 10.1007/s40195-017-0532-4.

[27]ASTM C876-15 Standard test method for corrosion potentials of uncoated reinforcing steel in concrete.

[28]Jovic, B.M.; Jovic, V.D.; Stratford G.R. Cyclic Voltammetry on Ag(111)and Ag (100)Facesin Sodium Hydroxide Solutions. Electrochem. Commun. **1999,** 1, 247-251.

[29]Zemlyanov, D.Y.; Savinova, E.; Scheybal, A.; Doblhofer, K.; Schlogl R. XPS Observation of OH Groups Incorporatedin an Ag(111) Electrode. Surf. Sci.**1998**, 418, 441-456.

[30]Duffo, G.S., Farina, S.B., Giordano, C.M., Characterization of Solid Embeddable Reference Electrodes for Corrosion Monitoring in Reinforced Concrete Structures. Electrochem. Acta. **2009**, 54, 1010-1020.

[31]Muralidharan, S., Ha, T.H., Bae,J.H.,Ha, Y.C., Lee, H.G., Kim, D.K. A Promising Potential Embeddable Sensor for Corrosion Monitoring Application in Concrete Structures. Measurement. **2007,** 40, 600-606.

[32]Gandía-Romero, J.M., Campos, I., Valcuende, M., García-Breijo, E., Marcos, M.D., Pay, J., Soto J. Potentiometric Thick-Film Sensors for Measuring the pH of Concrete. Cem. and Concr. Compos. **2016**, 68, 66-76.